

**NBSIR 77-1318**

# **The Impact of A Room Fire on A Corridor With Considerations of Fuel Load, Ventilation and Scaling**

---

J. Quintiere, B. McCaffrey, T. Kashiwagi, K. Den Braven,  
M. Harkleroad, J. Raines and W. Rinkinen

Center for Fire Research  
Institute for Applied Research  
National Bureau of Standards  
Washington, D.C. 20234

November 1977

Final Report



---

**U.S. DEPARTMENT OF COMMERCE**

**NATIONAL BUREAU OF STANDARDS**



NBSIR 77-1318

**THE IMPACT OF A ROOM FIRE ON  
A CORRIDOR WITH CONSIDERATIONS  
OF FUEL LOAD, VENTILATION AND  
SCALING**

---

J. Quintiere, B. McCaffrey, T. Kashiwagi, K. Den Braven  
M. Harkleroad, J. Raines and W. Rinkinen

Center for Fire Research  
Institute for Applied Research  
National Bureau of Standards  
Washington, D.C. 20234

November 1977

Final Report

**U.S. DEPARTMENT OF COMMERCE, Juanita M. Kreps, *Secretary***

**Dr. Sidney Harman, *Under Secretary***

**Jordan J. Baruch, *Assistant Secretary for Science and Technology***

**NATIONAL BUREAU OF STANDARDS, Ernest Ambler, *Acting Director***



## PREFACE

This work was begun in the summer of 1974. It was motivated by phenomena observed and recorded during previous tests of fire growth over floor coverings in building corridors. The fire scenario in those tests was a room fire spreading into a corridor. The potential for fire spread into the corridor would depend on the fire induced heating load in the corridor. Also the resultant flow pattern in the corridor could influence fire spread and smoke movement. The effect of room fire size, ventilation, geometry and other variables on the movement of smoke and energy from a room fire to a corridor would broaden the understanding of this fire scenario.

To accomplish this objective a series of full-scale experiments were conducted with the available room and corridor fire test facility at the former site of the National Bureau of Standards in Washington, D.C. (just before this site was abandoned). The scope of these experiments was to investigate the effect of the room fire, natural ventilation effects in the fire room, and the effect of an "obstruction" (floor fire or physical barrier) in the room doorway. Some of these data were used to provide a basis for comparison with corresponding results derived from a scale model (1/7th geometric scale) room and corridor facility. In this manner, the accuracy and limitations of scaling criteria could be evaluated, and the credibility of extrapolating results from scale model experiments could be assessed.

This report has been prepared to document and make available the results from the full-scale experiments and to present a complete set of results for the scaling experiments.



## CONTENTS

	<u>Page</u>
PREFACE . . . . .	iii
Abstract. . . . .	vi
INTRODUCTION. . . . .	vii
A SCALING STUDY OF A CORRIDOR SUBJECT TO A ROOM FIRE (ASME Preprint) . . . . .	1
COMPLETE SET OF SCALING RESULTS . . . . .	14
DESCRIPTION OF THE FULL-SCALE EXPERIMENTS . . . . .	46
CONCLUSIONS . . . . .	49

## Abstract

A study was conducted of heat transfer and temperature field imparted to a corridor by a room fire in order to assess the potential of fire spread along the corridor. Wood cribs were used as the fuel load which ranged from 20 to 120 kg. Also the effects of ventilation and fuel load location were examined. The results showed these effects to be significant.

A corresponding scale model study was conducted using gas burners as a fuel supply. A scaling criteria was developed which emphasized the solid wall conductive and gas phase convective transport processes. As a result limitations were encountered at high temperature when radiation became more significant. In general the convective processes appeared to scale well and radiation limitations could be assessed through analysis.

Key words: corridors; fuel load; heat transfer; room fires; scaling; ventilation.



## INTRODUCTION

This report will be based primarily on a presentation given at the ASME/AIChE 17th National Heat Transfer conference. A preprint of that presentation forms the main body of this text. This will be followed by a complete set of curves for all the scaling experiments. These show the comparison over time between the full-scale and model results. The results supplement those given in the preprint.

In the last section of this report, a description of the full-scale experiments will be given along with some general discussion. These data have not been analyzed extensively. The complete set of data is on the enclosed microfiche.

A SCALING STUDY OF A CORRIDOR SUBJECT TO A ROOM FIRE

(ASME Paper No. 77-HT-72)

(preprint follows)





**an ASME  
publication**

**\$3.00 PER COPY**

**\$1.50 TO ASME MEMBERS**

The Society shall not be responsible for statements or opinions advanced in papers or in discussion at meetings of the Society or of its Divisions or Sections, or printed in its publications. *Discussion is printed only if the paper is published in an ASME journal or Proceedings.*  
Released for general publication upon presentation.  
Full credit should be given to ASME, the Technical Division, and the author(s).

## **A Scaling Study of a Corridor Subject to a Room Fire**

**J. QUINTIERE**

**B. J. McCAFFREY**

Mechanical Engineers  
Mems. ASME

**T. KASHIWAGI**

Materials Engineer  
National Bureau of Standards,  
Washington, D.C.

A study was made of the thermal and flow environment within a corridor subject to a room fire of intensities of 300 to 1500 kW approximately. A corresponding model study was done under 1/7th geometric scale. Dimensionless groups were derived from the conservation equations governing the gas and solid phases. A subset of dimensionless groups was identified as significant to establish criteria to maintain partial dynamic scaling between the model and prototype experiments. Good results were achieved between the model and prototype for the convective process, i.e., gas temperature, velocity, and convective heat transfer. Radiant heat transfer did not scale, but an analysis of the data explains the lack of agreement in terms of dimensionless groups that were not preserved in scaling. A secondary result yielded corridor convective heat transfer coefficients which could be correlated by a general relationship.

Contributed by the Heat Transfer Division of The American Society of Mechanical Engineers for presentation at the AIChE-ASME Heat Transfer Conference, Salt Lake City, Utah, August 15-17, 1977. Manuscript received at ASME Headquarters April 20, 1977.

Copies will be available until May 1, 1978.



# A Scaling Study of a Corridor Subject to a Room Fire

J. QUINTIERE

B. J. McCAFFREY

T. KASHIWAGI

## ABSTRACT

A study was made of the thermal and flow environment within a corridor subject to a room fire of intensities of 300 to 1500 kW approximately. A corresponding model study was done under 1/7th geometric scale. Dimensionless groups were derived from the conservation equations governing the gas and solid phases. A subset of dimensionless groups was identified as significant to establish criteria to maintain partial dynamic scaling between the model and prototype experiments. Good results were achieved between the model and prototype for the convective process, i.e., gas temperature, velocity, and convective heat transfer. Radiant heat transfer did not scale, but an analysis of the data explains the lack of agreement in terms of dimensionless groups that were not preserved in scaling. A secondary result yielded corridor convective heat transfer coefficients which could be correlated by a general relationship.

## NOMENCLATURE

a absorption coefficient

A area

$c_p$  specific heat of gas-phase

$c_s$  specific heat of solid-phase

$C_0$  flow coefficient

$C_{1,2,3}$  constants of the fluid

d maximum doorway temperature ratio,  $T/T_\infty$

E energy flow rate

F configuration factor

g gravitational acceleration

Gr Grashof number,  $\frac{\rho_\infty^2 g k^3}{\mu^2}$

h heat transfer coefficient

$H_D$  height of doorway

$H_C$  height of ceiling

$\Delta H$  net heat of combustion

$H_f$  flame height

k thermal conductivity of gas-phase

$\ell$  length

$\bar{\ell}_g$  mean beam length of products

$\dot{m}$  mass flow rate

$\dot{m}_b$  rate of burning

p pressure relative to initial static pressure

Pr Prandtl number,  $\frac{\rho_\infty c_p}{k}$

$\dot{q}''$  rate of heat transfer per unit area

$\dot{q}_{Vol}$  energy release per unit volume

$\dot{Q}$  heat flow rate

r stoichiometric mass air to fuel ratio

Re Reynolds number,  $\frac{\rho_\infty V \ell}{\mu}$

t time

T temperature

u horizontal velocity component

v vertical velocity component

V velocity

W width

x horizontal coordinate

y vertical coordinate

Y concentration

$\alpha_g$  absorbtivity of the gas products

$\delta$  solid thickness

$\epsilon_s$  surface emissivity

$\kappa$  thermal diffusivity

$\mu$  viscosity

$\pi$  dimensionless group



$\rho$	density
$\sigma$	Stefan-Boltzmann constant

#### Subscripts

D	room doorway
E	corridor exit opening
FS	full-scale
M	model
r	radiation
R	reference
s	solid
$\infty$	initial

#### Superscripts

( )'	dimensionless
( $\bar{\phantom{x}}$ )	average

#### INTRODUCTION

A common approach used to study the spread and growth of fire and its effect on the surroundings has been to examine a particular fire scenario by using a small-scale model experiment. The obvious advantages of studying fire problems at a reduced size are less cost and ease of operation. However the problem with such an approach is the inability to maintain complete dynamic similarity between the prototype full-scale fire and the model. This would be evident by considering the paper of Williams (1) who lists no less than 28 dimensionless groups derived from the gas-phase conservation equations alone. Thus novel techniques and perceptive insight must be applied to fire problems, and the use of partial modeling must be employed. Thus perfection is not likely achieved in the "art" of fire modeling. Nevertheless valuable results can be achieved.

Scale model studies have been applied to an assortment of fire problems. Gross and Robertson (2) and Thomas (3) have used various size enclosures to study the rate of burning and other variables in fully-developed fires. These are generally fires which "fill" the enclosure, with flames extended out of the openings. Heskestad has done similar studies as well as modeling of sprinklered fires and the initial fire environment (4,5). The velocity and temperature fields have been studied for large mass ( $10^5 \text{ m}^2$ ) fires by Lee (6) and the plume above a house fire by Yokoi (7). The technique of conducting model studies at elevated pressures (in order to preserve buoyancy, inertia, and viscous effects) has been used by deRis, Kanury, and Yuen (8) for steady burning and by Alpert (9) for modeling transient wood crib fires. Parker and Lee (10) have used actual prototype room lining material and furnishing items to investigate the fire growth behavior in full and 1/4-scale rooms. All of these studies have yielded generally good results, but confidence in full-scale predictions from model results remains uncertain.

The study reported here was motivated by a desire to gain a greater understanding of factors influencing

corridor fire spread. Several years ago, experiments were conducted to study fire spread over floor covering materials in building corridors (11). The ignition source in this case was a room fire. These tests demonstrated that the fire produced conditions in the corridor had an ultimate effect on the nature of the fire spread over the floor covering material. In particular, radiant heat transfer to the floor was significant, but the significance of other factors, such as corridor flow patterns, initial fire size, or geometry, were not fully appreciated.

In order to more expeditiously explore these factors a scale model study was initiated. To provide a source of data for comparison with the model, a series of full-scale experiments were carried out to study the corridor flow and thermal conditions in terms of the room fire size. No floor covering flame spread was introduced in this work. These full-scale results would then serve as a basis for validating scale model results and thus could provide a measure of the accuracy of model results and scaling criteria. The scaling criteria were derived from the dominant set of dimensionless groups generated by conservation equations which best governed this problem. Ultimately the results could be applied to the development of mathematical models (12) for the prediction of corridor heat transfer to a room fire under general geometric, material, and ventilation constraints. Fire safety design analysis could then be applied to standards for selecting, for example, floor covering materials in corridors.

#### DIMENSIONAL ANALYSIS

The dimensionless groups for scaling were developed from the governing differential equations. Judgment was used in restricting the equations to include the significant thermal and fluid transport processes (e.g. viscous dissipation and pressure work terms were neglected). The transport of multicomponent gaseous species and the kinetics of combustion were totally ignored in this formulation. The effect of combustion was included through a heat generation term. This is justified since the field of interest in this problem was essentially outside the combustion zone. Also gas-phase radiation was neglected for simplicity in the gas-phase energy equation, but accounted for through a surface-to-gas boundary condition for the solid-phase energy equation. All thermodynamic and transport properties were considered constant except for density which follows an ideal gas law. Since the scaling laws ultimately derived will preserve temperature, and these properties are temperature dependent, the constant property assumption will not affect the derived dimensionless groups. With these restrictions the governing gas-phase dimensionless conservation equations follow. Without a loss in generality only the two-dimensional equations are presented.

#### Gas-Phase Equations

##### Mass

$$\left( \frac{\rho}{\rho_R} \right) \frac{\partial \rho'}{\partial t'} + \frac{\partial (\rho' u')}{\partial x'} + \frac{\partial (\rho' v')}{\partial y'} = 0 \quad (1)$$

### Momentum

$$\rho' \left[ \left( \frac{l}{V_R t_R} \right) \frac{\partial u'}{\partial t'} + u' \frac{\partial u'}{\partial x'} + v' \frac{\partial u'}{\partial y'} \right] = - \frac{\partial p'}{\partial x'} + \left( \frac{\mu}{\rho_\infty V_R l} \right) \left[ \frac{\partial^2 u'}{\partial x'^2} + \frac{\partial^2 u'}{\partial y'^2} + \frac{1}{3} \frac{\partial}{\partial x'} \left( \frac{\partial u'}{\partial x'} + \frac{\partial v'}{\partial y'} \right) \right] \quad (2)$$

$$\rho' \left[ \left( \frac{l}{V_R t_R} \right) \frac{\partial v'}{\partial t'} + u' \frac{\partial v'}{\partial x'} + v' \frac{\partial v'}{\partial y'} \right] = - \frac{\partial p'}{\partial y'} + \left( \frac{g l}{V_R^2} \right) (1 - \rho') + \left( \frac{\mu}{\rho_\infty V_R l} \right) \left[ \frac{\partial^2 v'}{\partial x'^2} + \frac{\partial^2 v'}{\partial y'^2} + \frac{1}{3} \frac{\partial}{\partial y'} \left( \frac{\partial u'}{\partial x'} + \frac{\partial v'}{\partial y'} \right) \right] \quad (3)$$

### Energy

$$\rho' \left[ \left( \frac{l}{V_R t_R} \right) \frac{\partial T'}{\partial t'} + u' \frac{\partial T'}{\partial x'} + v' \frac{\partial T'}{\partial y'} \right] = \left( \frac{k}{\rho_\infty c_p V_R l} \right) \left( \frac{\partial^2 T'}{\partial x'^2} + \frac{\partial^2 T'}{\partial y'^2} \right) + \left( \frac{l}{\rho_\infty c_p V_R T_\infty} \right) \dot{q}_{Vol} \quad (4)$$

### State

$$\rho' T' = 1 \quad \text{for enclosures with openings.} \quad (5)$$

The dimensionless variables have been defined as follows:

$$\rho' = \rho / \rho_\infty \quad (6)$$

where  $\rho_\infty$  is the initial density.

$$u' = \frac{u}{V_R} \quad \text{and} \quad v' = \frac{v}{V_R} \quad (7)$$

where  $V_R$  is a reference velocity that is determined by the observation that buoyancy should be of equal order of magnitude with the steady state inertia effect for

the fire problem addressed. Consequently from Eq. (3)

$$V_R \equiv \sqrt{g l} \quad (8)$$

where  $l$  is the geometric length scale (for example, the height of the corridor), and  $g$  is the gravitational acceleration.

$$T' = T / T_\infty \quad (9)$$

where  $T_\infty$  is the initial temperature.

$$p' = p / \rho_\infty V_R^2 \quad (10)$$

where  $p$  is the increase in pressure relative to the local initial hydrostatic pressure.

An expression for the energy release rate per unit volume,  $\dot{q}_{Vol}$ , depends on the volume of the combustion zone. One representation is given as

$$\dot{q}_{Vol} = \frac{\dot{m}_b(t) \Delta H}{l^3} \quad (11a)$$

where  $\dot{m}_b(t)$  is a known time dependent fuel production rate and  $\Delta H$  is the net heat of combustion. This representation is based on assuming complete combustion which occurs within a volume proportional to  $l^3$ . This may be reasonable for the application here since most of the visible flame zone is contained within the room, and for large fires flames tend to fill at least the upper volume of the room.

A more appropriate volume may be the flame volume itself. For flame heights less than that of the room height, this might be approximated by a cylinder of flame height,  $H_f$ , with a base area equal to the initial region where the fuel is introduced. Since turbulent flame height can be represented as (13)

$$H_f = 16 \left[ \frac{(r+\omega)^2 \omega}{\rho_\infty^2 g (1-\omega)} \right]^{1/5} \dot{m}_b^{2/5} \approx 16 \left[ \frac{r^2 \dot{m}_b^2 \omega}{\rho_\infty^2 g} \right]^{1/5}$$

$$\text{where } \omega = \frac{1}{1 + \frac{\Delta H}{r c_p T_\infty}} \approx \frac{r c_p T_\infty}{\Delta H} \sim 0(0.1)$$

this expression could be used to express a characteristic combustion volume as  $l^2 H_f$ . Hence an alternate expression to Eq. (11a) is

$$\dot{q}_{Vol} = \left[ \frac{(\dot{m}_b \Delta H)^{3/5} (\Delta H / r)^{3/5}}{16 l^2} \right] \left( \frac{\rho_\infty^2 g}{c_p T_\infty} \right)^{1/5} \quad (11b)$$

Time is normalized with a reference time  $t_R$  that should be characteristic of the fire behavior that is being studied. In the present study a characteristic time will be associated with the duration of the fire. This was approximately 30 minutes. Hence

$$t_R = \text{burnout time} \sim 30 \text{ minutes} \quad (12)$$

The dimensionless groups that then result from these equations are given below.

$$\pi_1 = \frac{1}{t_R} \sqrt{\frac{\ell}{g}} \sim \frac{\text{gas residence time}}{\text{burnout time}} \quad (13)$$

$$\pi_2 = \frac{\mu}{\rho_{\infty} g^{1/2} \ell^{3/2}} \sim \frac{\text{viscous force}}{\text{inertia force}} \quad (14)$$

$$\pi_3 = \frac{k}{c_p \rho_{\infty} g^{1/2} \ell^{3/2}} \sim \frac{\text{thermal conduction}}{\text{thermal convection}} \quad (15)$$

$$\pi_4 = \frac{\dot{m}_b \Delta H}{\rho_{\infty} c_p T_{\infty} g^{1/2} \ell^{5/2}} \sim \frac{\text{combustion energy}}{\text{thermal convection}} \quad (16a)$$

An alternate expression for  $\pi_4$  from Eq. (11b) is

$$\pi_4' = \left\{ \frac{(\dot{m}_b \Delta H) (\Delta H/r)}{\rho_{\infty} \sqrt{g} (c_p T_{\infty})^2 \ell^{5/2}} \right\}^{3/5} \quad (16b)$$

Thus scaling based on  $\pi_4$  over  $\pi_4'$  differs by a factor  $\Delta H/(rc_p T_{\infty})$ .

On examining the magnitude of these groups, it is found that for the full-scale corridor experiments of interest here

$$\begin{aligned} \pi_1 &\sim 0(10^{-3}), \\ \pi_2 &\sim \pi_3 \sim 0(10^{-6}), \\ \pi_4 &\sim 0(10^{-1}). \end{aligned}$$

These estimates were based on  $\ell$  taken as the corridor height. Consequently, it will be assumed that terms in the equations can be neglected which have coefficients of  $\pi_1$ ,  $\pi_2$ , or  $\pi_3$ . The physical significance of these deletions follows: (1) The gas-phase is quasi-steady with burning rate contained in  $\pi_4$  as the time-dependent "driving force." The time for fluid to be transported through the corridor is considered short compared with changes in the burning rate. Also regular flow oscillations and turbulence are contained in the unsteady terms, and thus are not considered explicitly. (2) The viscous and thermal conduction effects are ignored near solid boundaries. This will have to be compensated for later when considering the transfer of heat at solid boundaries. It can be shown that  $\pi_2$  and  $\pi_3$  may be redefined as

$$\pi_2 \equiv 1/\sqrt{Gr} \quad (17)$$

and

$$\pi_3 \equiv 1/Pr\sqrt{Gr} \quad (18)$$

where  $Gr$  is a Grashof number and  $Pr$  is a Prandtl number. In this scaling study the  $Gr$  will be greater than  $10^9$  for both the model and full-scale system which should insure turbulent flow. This would imply that turbulent mixing away from solid boundaries is independent of scale.

### Solid-Phase Equations

In order to complete the derivation of the significant dimensionless groups, heat transfer at solid boundaries needs to be considered. Also in the solid-phase formulation, the radiative exchange with the layer of combustion products must be included. This will be done by characterizing the gas at a single temperature,  $T$ .

For illustration, an inert solid of thickness  $\delta$  is considered heated by a hot finite layer of combustion products at temperature  $T$  which is bounded below by cold black surroundings at  $T_{\infty}$ . This is representative of the corridor ceiling. The conduction equation is given as

$$\frac{\partial T_s}{\partial t} = \kappa_s \frac{\partial^2 T_s}{\partial x_s^2} \quad (19)$$

where  $\kappa_s$  is the solid thermal diffusivity. An internal boundary condition has the form

$$x_s = 0: -k_s \frac{\partial T_s}{\partial x_s} = h(\bar{T} - T_s) + \dot{q}_r'' \quad (20)$$

where  $k_s$  is the thermal conductivity

$h$  is the convective heat transfer coefficient

and  $\dot{q}_r''$  is the net radiant flux to the surface.

The radiative flux can be represented as

$$\dot{q}_r'' = \epsilon_s (1 - \alpha_g) \sigma (T_{\infty}^4 - T_s^4) + \epsilon_s \alpha_g \sigma (\bar{T}^4 - T_s^4) \quad (21)$$

Here  $\epsilon_s$  is the surface emissivity and  $\alpha_g$  is the absorptivity of the gas layer which may be represented as

$$\alpha_g \sim 1 - e^{-a\ell_g} \quad (22)$$

where  $a$  is the absorption coefficient and  $\ell_g$  is a characteristic mean beam length.

It is reasonable to expect that  $\ell_g \sim 0(\ell)$ . It should be noted that Eq. (21) does not contain geometric shape factors for surface to surface radiative change, and in fact applies to radiative exchange between infinite parallel plates. In general, the shape factors must be regarded as additional dimensionless groups which will automatically be satisfied if geometric similarity is maintained.

The convective heat transfer coefficient in Eq. (20) must be a function of scale and therefore must be represented by an appropriate relationship. Since the nature of fire induced flow within an enclosure has been perceived as consisting of a cold floor jet and hot ceiling jet,  $h$  is derived from a constant property turbulent boundary layer correlation for flow over a flat plate.



$$h = \frac{C_1 k}{\ell} \text{Re}^{0.8} \quad (23)$$

where  $C_1$  is a constant for a given fluid,  $0.036 \text{ Pr}^{1/3}$ , and  $\text{Re}$  is the Reynolds number represented as

$$\text{Re} = \frac{\rho_\infty V \ell}{\mu} = \frac{\rho_\infty \sqrt{g} \ell^{3/2}}{\mu} \quad (24)$$

By combining Eqs. (19) through (24) and making terms dimensionless the following results:

$$\pi_5 \frac{\partial T'_s}{\partial t'} = \frac{\partial^2 T'_s}{\partial x'^2} \quad (25)$$

$$x'_s = 0 : -\frac{\partial T'_s}{\partial x'_s} = \pi_6 (\bar{T}' - T'_s) + \pi_7 (1 - \pi_8) (1 - T'^4_s) + \pi_7 \pi_8 (\bar{T}'^4 - T'^4_s). \quad (26)$$

The dimensionless groups are

$$\pi_5 = \frac{\delta^2}{\kappa_s t_R} \sim \frac{\text{thermal penetration time}}{\text{burnout time}} \quad (27)$$

$$\pi_6 = \frac{C_2 \ell^{0.2} \delta}{k_s} \sim \frac{\text{convective heating}}{\text{solid conductive heating}} \quad (28)$$

where  $C_2$  is a fluid dependent parameter,

$$\pi_7 = \frac{\epsilon_s \sigma T_\infty^3 \delta}{k_s} \sim \frac{\text{surface radiative heating}}{\text{solid conductive heating}} \quad (29)$$

$$\pi_8 = \alpha_g = 1 - e^{-(a\ell)(\ell_g/\ell)} \quad (30)$$

It should be pointed out that the above groups  $\pi_5 - \pi_8$  hold for a solid boundary in which  $t_R \geq \delta^2/\kappa_s$ . This means that the thickness  $\delta$  is significant and the effects of heating are significantly felt throughout the solid. Also the above groups apply to all gas-solid interfaces since they all would have a boundary condition similar to Eq. (20).

However for thermally thick solids and for composite solids, an alternative set of dimensionless groups apply. These are summarized below:

Thermally thick solid boundary,  $t_R \ll \delta^2/\kappa_s$

$$\pi'_s = \begin{cases} \pi_5/\pi_7^2 = \frac{(k\rho c)_s}{t_R (\epsilon_s \sigma T_\infty^3)^2} \\ \pi_6/\pi_7 = \frac{C_2 \ell^{0.2}}{\epsilon_s \sigma T_\infty^3} \\ \pi_8 \end{cases} \quad (31)$$

Composite solid with layers A and B,  $t_R \geq (\delta^2/\kappa_s)$  for A and B

$$\pi'_s = \begin{cases} \pi_5 & \text{through } \pi_8 \text{ for solid A} \\ \pi_9 = \left( \frac{\delta^2/\kappa_s}{t_R} \right)_B \\ \pi_{10} = (k_s \rho_s c_s)_A / (k_s \rho_s c_s)_B \end{cases} \quad (32)$$

Composite solid with thick second layer,  $t_R \ll (\delta^2/\kappa_s)_B$

$$\pi'_s = \begin{cases} \pi_5 & \text{through } \pi_8 \text{ for solid A} \\ \pi_{10} \end{cases} \quad (33)$$

#### Scaling Criteria

In order to achieve exact similarity between a model and prototype all the appropriate dimensionless groups must be preserved in scaling. Indeed, the set of groups presented here is only a partial set since some restrictions have been made. Yet even this partial set is too numerous to achieve complete preservation. Thus a sub-set of the groups will be selected in order to design a model. It has already been pointed out that for this application  $\pi_1$ ,  $\pi_2$ , and  $\pi_3$  can be neglected. Also in designing a reduced size model it is impossible to preserve  $\pi_6$  and  $\pi_7$  simultaneously unless  $\epsilon_s$  is manipulated in order to obtain agreement between the model and the prototype. It would be difficult to control surface emissivity appropriately especially since soot is likely to coat the heated surfaces in these fire experiments. In fact  $\epsilon_s$  was held the same by painting the walls and ceiling of the corridor with a high temperature resistant black paint. Thus, the rationale is to favor  $\pi_6$  if convection is significant, and favor  $\pi_7$  if radiation is important. Finally it is also impossible to accomplish similarity for flame or gas radiation, and  $\pi_8$  will be ignored in designing a model.

In summary, the following groups will be preserved in scaling (within the limits of material constraints):

$$\pi_4 = \frac{\dot{m}_b(t) \Delta H}{\rho_\infty c_p T_\infty g^{1/2} \ell^{5/2}},$$

$$\pi_5 = \frac{\delta^2}{\kappa_s t_R},$$

$$\pi_6 = \frac{C_2 \ell^{0.2\delta}}{k_s} \quad \text{or} \quad \pi_7 = \frac{\epsilon_s \sigma T_\infty^3 \delta}{k_s}$$

and  $\pi_9$  and  $\pi_{10}$  if necessary. It is implicit that geometric similarity must also be preserved. As a result of these scaling criteria, the dependent variables will scale as follows:

$$(\text{temperature}) \quad T_M = T_{FS} \quad (34)$$

$$(\text{velocity}) \quad V_M = \sqrt{\frac{\ell_M}{\ell}} \cdot V_{FS} \quad (35)$$

(floor incident radiant flux)

$$\dot{q}_M'' = \dot{q}_{FS}'' \quad (\text{if } \pi_7 \text{ \& } \pi_8 \sim 0) \quad (36)$$

at the same time and corresponding coordinates. Since approximations introduced in arriving at this scaling criteria have been based on judgment and physical constraints, the results will indicate the accuracy of relationships (34)-(36).

The internal dimensions of the room-corridor model were selected to be 1/7th of full-scale. This geometric scale was selected for its convenient overall size relative to our laboratory space yet large enough in height to give a  $Gr \geq 10^9$  to insure turbulent flow. The construction and lining materials were selected according to the dimensionless groups and available materials. The extent to which the dimensionless groups were preserved is shown in Table 1. Table 2 lists the materials and some of their properties. It is apparent from Table 1 that perfect agreement of the dimensionless groups could not be achieved. This was due to the unlikely prospect of finding available materials to meet the exact model requirements in size and properties. For the walls and ceiling linings an attempt was made to match  $\pi_5$  and  $\pi_6$ ; thus,  $\pi_7$  was uncontrolled. The outer material

on the room walls and ceiling was not considered very important within the duration of these fires. Therefore  $\pi_9$  would be irrelevant for the thermally thick outer layer, but  $\pi_{10}$  would be significant. For the floor, which was expected to be a cold thermal sink for radiation, agreement among the dimensionless groups was considered rather loosely. In fact, as opposed to the results in Table 1, the floor was considered to be a semi-infinite layer of asbestos cement board (which has properties similar to brick). Under this approximation the group  $\pi_5/\pi_7^2$  is preserved.

## EXPERIMENTAL DESIGN AND PROCEDURE

### Full-Scale

In this series, nine experiments were conducted. The effects of room fire fuel loading, location, and ventilation were examined in the series. Only the five experiments in which room fuel loading was varied will be considered in this report. The room was 2.6 m x 2.4 m x 2.8 m high with a single opening, a doorway 2.0 m high x 0.79 m wide, leading to the corridor. The corridor was 2.44 m x 2.44 m x 9.14 m long with a window at one end which was 0.66 m above the floor and 1.7 m high x 1.0 m wide. The window was oriented at a corner and was connected to the outside by a 1. m long duct. The instrumentation consisted of 53 Chromel-Alumel 0.25 mm thermocouples (T), five total heat flux (H) and radiant heat flux (R) sensors, eight pitot-static tubes (P) monitored by variable reluctance pressure transducers, and five electrolytic oxygen cells (O). The overall layout of these probes is shown in Figure 1. The heat flux sensors were water-cooled thermopile sensing elements coated with an 0.96 emissivity paint. The radiometers had their sensing element shielded by a CaF<sub>2</sub> window scrubbed continuously by small air jets. These heat flux sensors were calibrated at the start and end of the test series. A shift in calibration was generally within 5% except for H5 (20%) which was cleaned and repainted after the first test and R5 was ignored since its window broke. The radiometers were not

Table 1. - Dimensionless groups\*

		$\pi_5 = \frac{\delta^2}{\kappa_s t_R}$	$\pi_6 = \frac{C_2 \ell^{0.2\delta}}{k_s}$	$\pi_7 = \frac{\epsilon_s \sigma T_\infty^3 \delta}{k_s}$	$\pi_9 = \left( \frac{\delta^2}{\kappa_s t_R} \right)$ OUTER LAYER	$\pi_{10} = \frac{(k\rho c)_s, \text{ INNER}}{(k\rho c)_s, \text{ OUTER}}$
Corridor Walls and Ceiling	Full-scale Model	0.85 1.1	3.3 4.3	0.13 0.24	-- --	-- --
Room Walls and Ceiling	Full-scale Model	0.93 1.60	9.2 11.0	0.35 0.62	38.0 1.1	0.021 0.087
Floor	Full-scale Model	0.046 0.73	0.21 0.58	0.0081 0.032	4.8 --	2.0 --

\* Notes: (1)  $t_R = 0.5$  hr, (2)  $\epsilon_s = 1$ , (3)  $T_\infty = 295$  K.

Table 2. - Lining materials and their properties

	Thickness	$k_s$	$c_s$	$\rho$	$\kappa_s$	$(k\rho c)_s$
	cm	W/(m-K)	kJ/(kg-K)	kg/m <sup>3</sup>	10 <sup>-6</sup> m <sup>2</sup> /s	kJ <sup>2</sup> /(m <sup>4</sup> -K <sup>2</sup> -s)
<b>CORRIDOR WALLS AND CEILING -</b>						
Full-scale: Gypsum board	1.6	0.17	1.1	960	0.17	0.18
Model: Calcium silicate board	1.9	0.11	1.0	580	0.18	0.066
<b>ROOM WALLS AND CEILING -</b>						
<u>Inner Lining:</u>						
Full-scale: Spray coated insulation	2.5	0.099	0.84	300	0.39	0.025
Model: Alumina-silica block	2.5	0.056	1.0	240	0.22	0.014
<u>Outer Lining:</u>						
Full-scale: Concrete block	18	0.73	0.84	1900	0.46	1.2
Model: Plywood	1.3	0.12	2.5	540	0.085	0.16
<b>FLOOR -</b>						
<u>Inner Lining:</u>						
Full-scale: Asbestos-cement board	0.64	1.1	1.0	2100	0.49	2.3
Model: Asbestos-cement board	2.5	1.1	1.0	2100	0.49	2.3
<u>Outer Lining:</u>						
Full-scale: Brick	6.4	0.73	0.84	1900	0.46	1.2
Model: None	--	--	--	--	--	--

to 13%. The mass loss of the fuel during combustion was monitored by means of a platform suspended from a strain-gage load cell transducer which was in a cooled container above the room. In the five experiments presented here, the cribs were centered on the platform which was approximated 15 cm above the floor. The fuel loading varied from one to five cribs through the five tests. The cribs were ignited by pans of heptane and generally burned to a less than 10% ash residue in 30 minutes.

The series of five experiments presented here were run over a two week period during evenings in the spring. The same gypsum board lining material was used throughout the tests, however, an earlier experiment damaged a section of the ceiling near the room doorway. This section was covered with a 2 m x 1 m x 1 cm sheet of asbestos mill board (930 kg/m<sup>3</sup>) for added protection. It should be pointed out that this earlier test produced ceiling temperatures of 200°C to 500°C which should have been sufficient to remove the water of hydration (20% by mass) of the gypsum board ceiling. Thereafter only absorbed moisture of up to 5% may have been present in the gypsum board. This moisture content is comparable to that of the asbestos cement board used in the model.

#### Model

The model was constructed of the materials described in Table 2 with internal dimensions equal to 1/7th full-scale. In order to validate scaling, it was felt that only selected data would need to be recorded. Four 0.12 mm Chromel-Alumel thermocouples each recorded the vertical temperature distribution in the room doorway, corridor, and exit window. Three additional thermocouples monitored corridor ceiling temperature. Flush mounted water-cooled total heat flux sensors measured incident flux at three positions along the

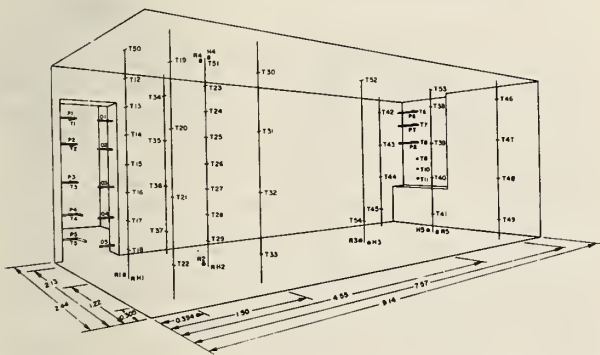


Fig. 1 Corridor geometry and instrumentation for full-scale experiments (distances in metres) T- thermocouples, R- radiometer, H- total heat flux, P- pitot static tube, O- oxygen concentration.

generally useful since the CaF<sub>2</sub> has a transmissivity which falls off to zero at 12μm which leads to a 25% error or greater for source temperatures below 400°C. The oxygen cells and pressure transducers were calibrated before each run.

The fuel burned was cribs of Hemlock made of 3.8 cm x 3.8 cm square sticks spaced 7.6 cm apart in 16 layers with 4 sticks per layer. Each crib weighed approximately 19 kg and had a moisture content of 10



floor and one location at the ceiling. Two pitot-static probes were used to derive the exit flow velocity at the window. All of these sensors were located at positions corresponding to their counterpart in the full-scale experiment.

In both the model and full-scale, data were recorded on a high-speed multi-channel analog-digital acquisition system at a record rate of every 10 seconds for 30 minutes.

The fire source in the model was four water-cooled brass diffusion flame burners centered above the floor of the room. They were sized and located according to 1/7th geometric scaling relative to the height and cross-sectional area of a wood crib. The burner height was 5.5 cm above the floor and had a coarse screen covered port diameter of 6 cm. The fuel was methane ( $\text{CH}_4$ ) metered through a high and low capacity rotometer. The criterion for establishing the correlating flow rate was  $\pi_{14}$  given by Eq. (16a). That is,

$$\dot{m}_{\text{CH}_4, \text{M}} = \dot{m}_{\text{WOOD CRIB}} \times \left[ \frac{(\Delta H)_{\text{WOOD}}}{(\Delta H)_{\text{CH}_4}} \right] \times \left[ \frac{\ell_{\text{M}}}{\ell_{\text{FS}}} \right]^{5/2} \quad (37)$$

where  $(\Delta H)_{\text{WOOD}} = 16.3 \text{ MJ/kg}$  for Hemlock with 12% moisture, and  $(\Delta H)_{\text{CH}_4} = 50.0 \text{ MJ/kg}$ . The burning rate was determined by taking a five-point derivative of the crib mass loss data and averaging this over 100 second intervals. Then the  $\text{CH}_4$  flow rate was manually controlled in the model experiments over corresponding 100 second intervals. The number of burners was equal to the number of cribs burned in a given experiment except four burners were used to simulate the five crib case. From the relationship for free burning turbulent flame height (13) it follows that

$$\frac{H_{f, \text{FS}}}{H_{f, \text{M}}} \cong 0.8 \left( \frac{\ell_{\text{FS}}}{\ell_{\text{M}}} \right) \quad (38)$$

Thus, geometric scaling of flame heights will not be achieved. This distortion would even be greater for flames that impinge and extend under a ceiling.

## RESULTS

### General Observations

More smoke appeared to be produced in the full-scale crib fires than in the model experiments. In fact for 3 or more cribs dark grey smoke obscured vision along the corridor. Also fire brands from the wood cribs were generated in all fuel loadings and their trajectory followed the jet of combustion products which issued from the room. The corresponding flame lengths were longer in the model fires. In the 5 crib full-scale burns, flames scrubbed the corridor wall opposite the room doorway. However, in the corresponding model case, flames extended to thermocouple T23. The pressure transducers used in the full-scale experiments were later found to have had problems with zero drift and did not yield consistently reliable results. Despite this problem, it was deduced that the mass flow rates were  $0.75 \pm 0.25 \text{ kg/s}$  for the doorway and  $1.0 \pm 0.2 \text{ kg/s}$  for the window; generally, independent of fuel loading. The lowest oxygen con-

centration (dry gas basis) for the room fire products occurred for 5 cribs and was recorded at 3 per cent (sensor 01). The average peak burning rates ranged from 18 to 92 g/s, roughly 18 g/s per crib. None of these fires were ventilation (air) limited.

### Typical Scaling Comparisons

Selected channels of data were compared directly for the model and full-scale results. The two sets of data were processed and plotted by a computer. As a representative example, the 3 crib fuel loading case will be presented. The "input function" for scaling was the rate of burning for the cribs. The resultant mass loss for 3 cribs is shown in Figure 2 along with

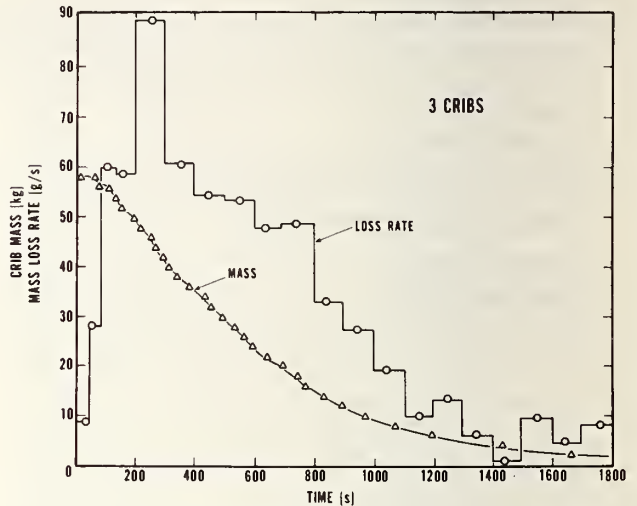


Fig. 2 Mass and mass loss rate for the 3 crib full-scale experiment.

the rate function prescribed in the model. The erratic rate behavior at the end of burning was probably caused by cribs collapsing. Temperature comparisons are shown in Figures 3 through 6 for the room doorway, corridor vertical traverse at 1.5 m (5 ft.), the exit window, and the ceiling, respectively. In general, the results were poorest for the ceiling temperature. As a consequence, the radiation heat transfer to the floor, shown in Figure 7, is also lacking in agreement. The full-scale window velocity data was the most reliable and therefore that was compared to the model results. These data compare favorably (Fig. 8) except perhaps for a "drift" problem in full-scale V7. Also shown in Figure 8 is a ceiling heat transfer coefficient (HTC 4) determined at 1.5 m. This was defined as

$$h \equiv \frac{\dot{q}_{14}}{T_g - T_w} \quad (39)$$

where  $\dot{q}_{14}$  is the measured flux by sensor H4,  $T_g$  is the gas temperature measured by T23, and  $T_w$  is  $22^\circ\text{C}$ , the temperature of the water-cooled sensor. The ceiling flux data was not corrected for radiation, and consequently an overestimate in  $h$  of up to 30 per cent in full-scale could result. It follows from Eq. (23) and

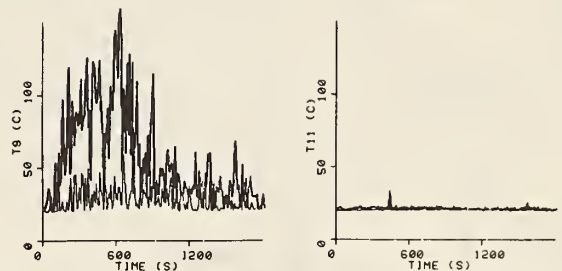
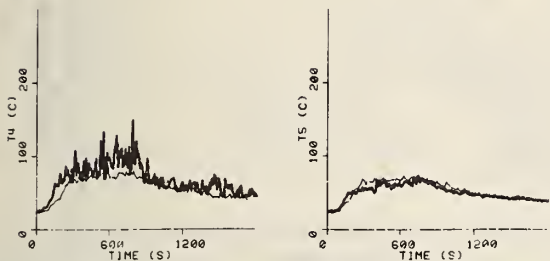
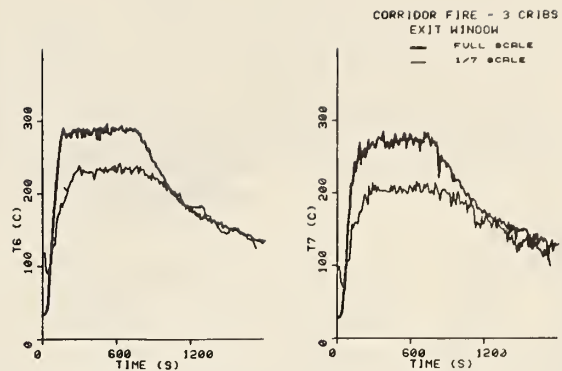
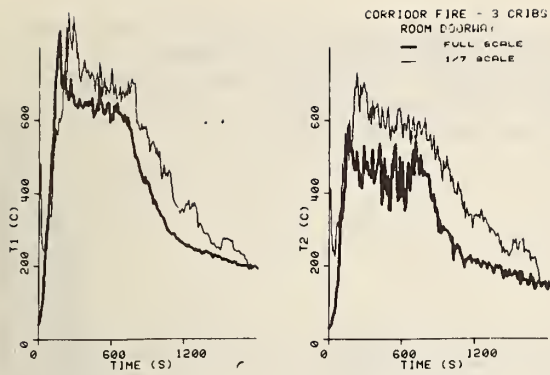


Fig. 3 Room doorway temperatures for model and full-scale experiments (3 cribs).

Fig. 5 Exit window temperatures for model and full-scale experiments (3 cribs).

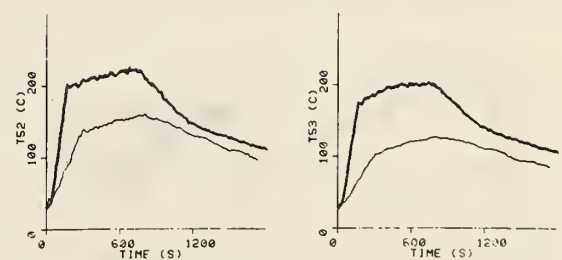
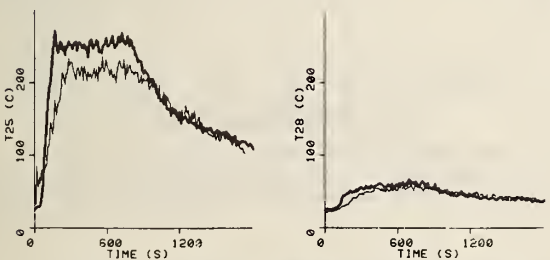
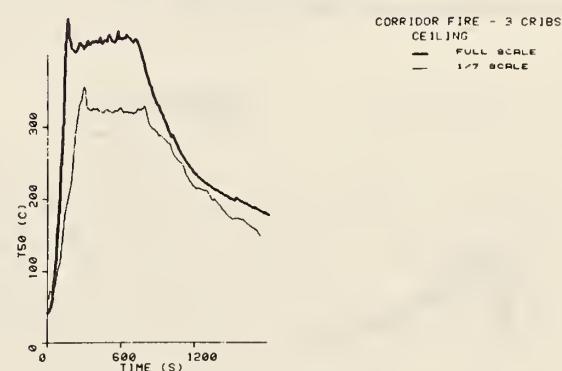
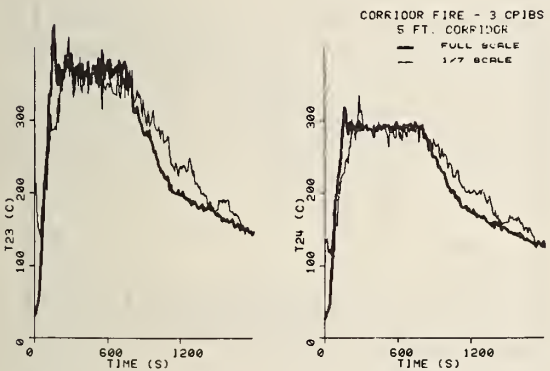


Fig. 4 Corridor vertical temperature distribution for model and full-scale experiments (3 cribs).

Fig. 6 Corridor ceiling temperatures for model and full-scale experiments (3 cribs).

(24) that the scaling factor for  $h$  was  $\ell^{0.2}$  which was applied to the model values for  $h$  in Figure 8.

Overall results for the fire scaling experiments are compared in Figures 9 through 11. Figure 9 displays corridor vertical temperature distributions

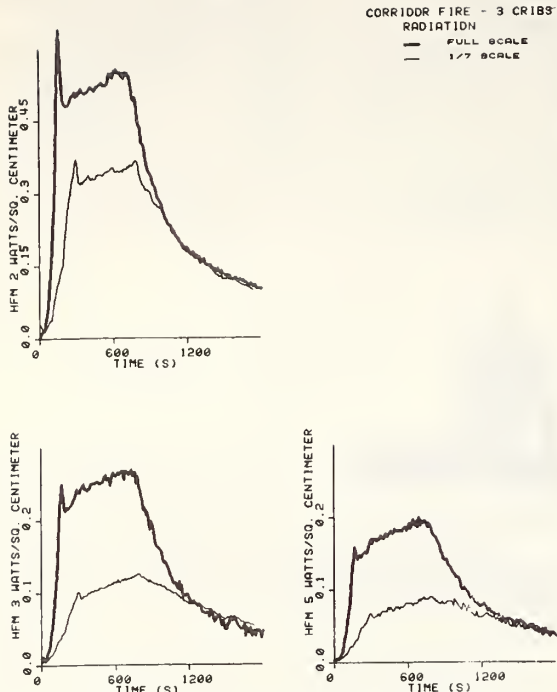


Fig. 7 Corridor floor irradiance for model and full-scale experiments (3 cribs).

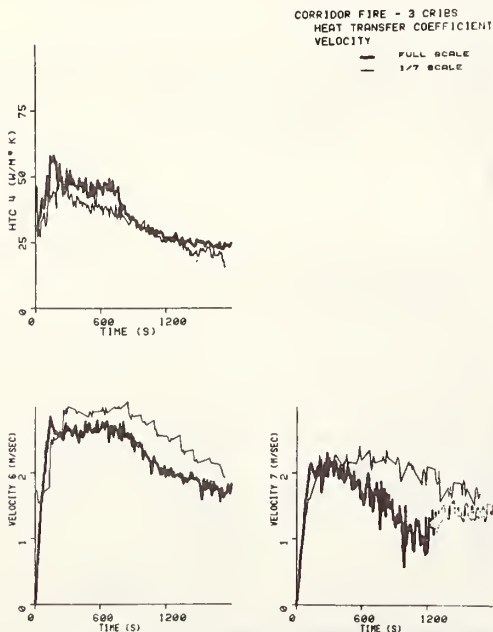


Fig. 8 Corridor ceiling heat transfer coefficient and exit window velocities for model and full-scale experiments (3 cribs). Note:  $h$  (HTC 4) for model was scaled to full-scale by multiplicative factor of  $7^{0.2}$ .

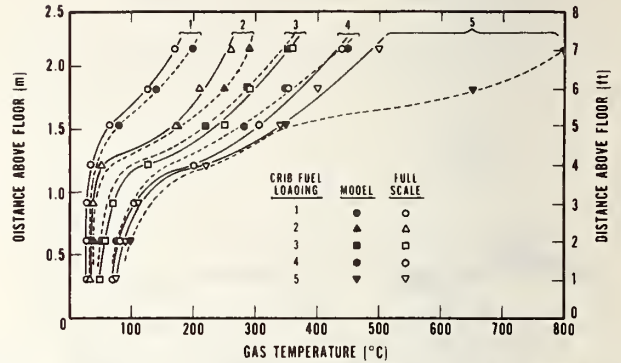


Fig. 9 Average maximum corridor vertical gas temperatures for various room fire sizes and for model and full-scale experiments.

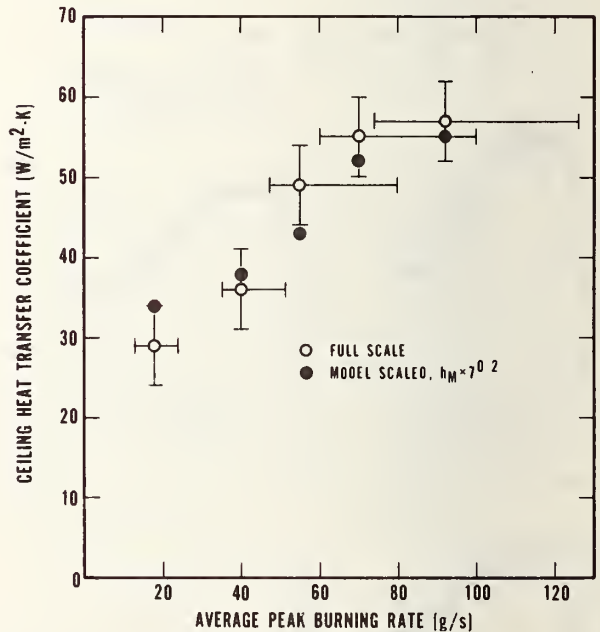


Fig. 10 Comparison of full-scale and scaled model ceiling heat transfer coefficients as a function of full-scale burning rate.



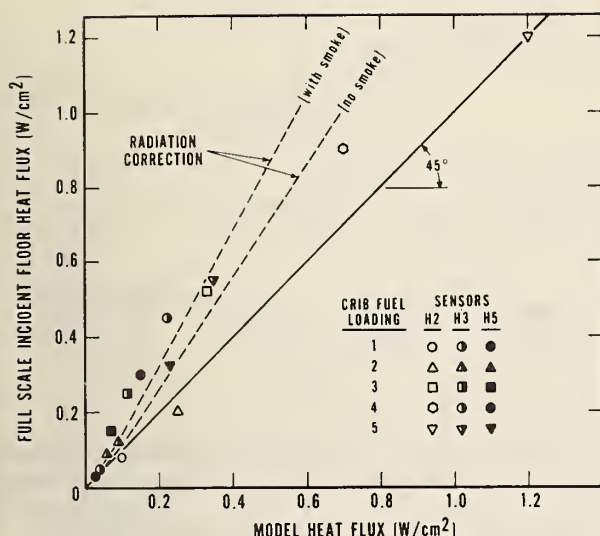


Fig. 11 Comparison of full-scale and model floor irradiance at maximum steady burning.

for the T23 thermocouple traverse during peak burning rates. The higher gas temperatures in the model for the 5 crib case were the result of flames extending to those thermocouples. This was a distortion in flame length between model and full-scale. Figure 10 displays the convective heat transfer coefficient scaling results in terms of the peak crib burning rates. The bars on the full-scale results indicate the range during maximum "steady" burning conditions. Finally, Figure 11 compares the incident floor radiative heat flux for the model and full-scale at average peak burning as derived from the nearly flat portion of the flux curves in Figure 7. As shown, the model flux values are generally lower than the full-scale corresponding values. The reason for this can be traced back to the lack of preservation in the radiation groups  $\pi_7$  and  $\pi_8$ . This can be quantitatively demonstrated by the following analysis.

#### ANALYSIS

Better agreement may be achieved for the floor flux scaling results, or their differences may be explained by applying a correction factor to the data which accounts for differences in  $\pi_7$  and  $\pi_8$  (as well as  $\pi_6$ ). This was done by assuming no conduction loss to the ceiling during peak burning, and considering a ceiling heat balance from Eq. (26)

$$0 = \pi_6 (\bar{T}' - \bar{T}_s') + \pi_7 (1 - \pi_8) (1 - \bar{T}_s'^4) + \pi_7 \pi_8 (\bar{T}'^4 - \bar{T}_s'^4). \quad (40)$$

The dimensionless radiative flux to the floor can be expressed as

$$\frac{\dot{q}''}{\epsilon_s \sigma T_\infty^4} = (1 - \pi_8) \bar{T}_s'^4 + \pi_8 \bar{T}'^4 \quad (41)$$

where the configuration factor was ignored and  $\epsilon_s$  was taken as 1. These two equations can be solved for  $\bar{T}'$  in terms of  $\bar{T}_s'$  for values of  $\pi_6$  and  $\pi_7$  given in Table 1, and  $\pi_8$  taken as 0.11 for the model and 0.25 for full-scale based on no smoke and characteristic  $\text{CO}_2$  and  $\text{H}_2\text{O}$  concentrations of 10 per cent each and a beam length of 1 m. Since smoke was more apparent in full-scale,  $\pi_8$  was estimated as 0.50 to account for smoke. The correction factor or correlating curve was then determined by solving for

$$\left[ \frac{(\dot{q}'')_{\text{FULL-SCALE}}}{(\dot{q}'')_{\text{MODEL}}} \right] \bar{T}' = \text{constant} \quad (42)$$

where  $\bar{T}'$  was based on T23 (from Figure 9). This factor was applied to the model data of H2 and H3 to yield the curves in Figure 11.

In analyzing the ceiling heat transfer coefficient results, it appeared that the turbulent flat plate correlation was valid, and that room or doorway temperature affected the results. It is believed that the maximum doorway jet velocity controls the convective corridor ceiling heating at least near the doorway (perhaps for distances within a door height,  $H_D$ ). This velocity can be ideally expressed as (14)

$$V = C_0 \sqrt{2gH_D} \left[ \frac{1-d}{d(1+d^{1/3})} \right]^{1/2} \quad (43)$$

where  $d$  is the temperature ratio  $T/T_\infty$ ,

$H_D$  is the door height,

and  $C_0$  is a flow coefficient (0.7).

Substituting this expression for  $V$  into Eq. (23) and taking  $l = H_D$ , it follows that

$$h = C_3 c_p (4g^2 \rho^4 C_0^4 \mu) \cdot H_D \cdot \left[ \frac{1-d}{d(1+d^{1/3})} \right]^{0.4} \quad (44)$$

where  $C_3$  is a constant for the fluid. Taking  $T$  as doorway temperature  $T_l$  and evaluating fluid properties at normal room temperature the results of this correlation are presented in Figure 12. The data were derived from quasi-steady periods during the scaling experiments. Also plotted there are results for other model tests which had various width exit doorways instead of the window used in the scaling series.

Finally an approximate energy balance was done for the full-scale 3 crib fire condition. This analysis assumed a nominal air flow of 1 kg/s, and considered the average peak burning period only. A sketch of the analysis follows:

$$\begin{aligned} \left[ \begin{array}{c} \dot{E} \\ \text{COMBUSTION} \end{array} \right] & \text{(by mass loss)} = \dot{m}_b \Delta H_{\text{Wood}} \\ & = (55 \text{ g/s})(16 \text{ kJ/g}) = 880 \text{ kW} \end{aligned}$$

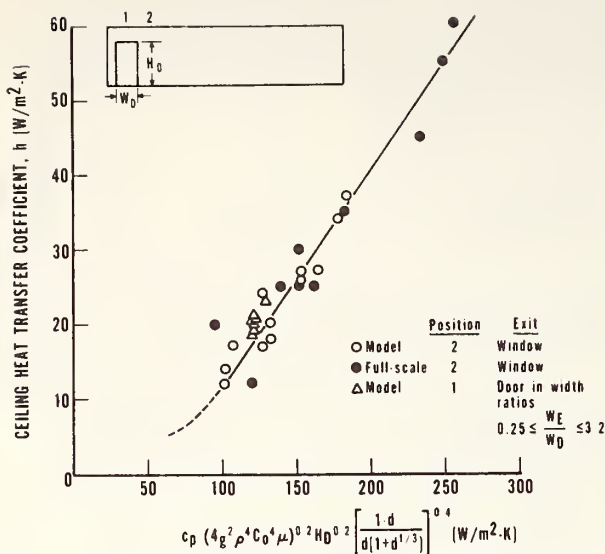


Fig. 12 A correlation for ceiling heat transfer coefficient.

$$\begin{aligned} \left[ \begin{array}{c} \cdot \\ E \end{array} \right] \text{ COMBUSTION (by } O_2 \text{ depletion)} &= \dot{m}_{\text{air}} \Delta Y_{O_2} \Delta H_{O_2} \\ &= (1 \text{ kg/s}) (0.21-0.14) \left( 13240 \frac{\text{kJ}}{\text{kg}} \right) = 927 \text{ kW} \end{aligned}$$

$$\begin{aligned} \left[ \begin{array}{c} \cdot \\ E \end{array} \right] \text{ DOORWAY ENTHALPY} &= \dot{m}_{\text{air}} c_p \Delta T = (1 \text{ kg/s}) (1.05 \frac{\text{kJ}}{\text{kg-K}}) \\ (520 \text{ K}) &= 520 \text{ kW} \end{aligned}$$

$$\begin{aligned} \left[ \begin{array}{c} \cdot \\ Q \end{array} \right] \text{ DOORWAY RADIATION} &= \sigma T^4 A = \left( 5.7 \times 10^{-11} \frac{\text{kW}}{\text{m}^2 \cdot \text{K}^4} \right) \\ (810 \text{ K})^4 (1 \text{ m}^2) &= 25 \text{ kW} \end{aligned}$$

$$\begin{aligned} \left[ \begin{array}{c} \cdot \\ Q \end{array} \right] \text{ CORRIDOR CONVECTION TO CEILING \& WALLS} &= hA(\bar{T} - \bar{T}_s) \\ &= \left( 0.045 \frac{\text{kW}}{\text{m}^2 \cdot \text{K}} \right) (50 \text{ m}^2) (370-315) \\ &= 124 \text{ kW} \end{aligned}$$

$$\begin{aligned} \left[ \begin{array}{c} \cdot \\ Q \end{array} \right] \text{ CORRIDOR RADIATION FROM CEILING \& WALLS TO GAS} &= \left[ (1-\alpha_g) \sigma \bar{T}_s^4 - \alpha_g \sigma (\bar{T} - \bar{T}_s)^4 \right] A \\ &= 219 \text{ kW for } \alpha_g = 0.25 \\ &= 97 \text{ kW for } \alpha_g = 0.5 \end{aligned}$$

$$\begin{aligned} \left[ \begin{array}{c} \cdot \\ Q \end{array} \right] \text{ RADIATION FROM HOT LAYER TO FLOOR} &= \frac{1}{F} \sum_{i=1}^4 \dot{q}_{r,i} A_i \\ &= \left( \frac{1}{0.5} \right) \left( \frac{2.4 \times 9.1}{4} \text{ m}^2 \right) \\ &\quad \left( 7+5+2.2+1.8 \frac{\text{kW}}{\text{m}^2} \right) = 175 \text{ kW} \end{aligned}$$

$$\begin{aligned} \left[ \begin{array}{c} \cdot \\ E \end{array} \right] \text{ WINDOW ENTHALPY} &= \dot{m}_{\text{air}} c_p \Delta T = (1 \text{ kg/s}) \left( 1.05 \frac{\text{kJ}}{\text{kg-K}} \right) \\ (250 \text{ K}) &= 250 \text{ kW} \end{aligned}$$

Thus about two-thirds of the energy released in the room reaches the corridor, and more than half of that energy is lost in the corridor. Admittedly these results are very approximate, and only serve to give an order of magnitude of the flow of energy in the corridor.

#### DISCUSSION AND CONCLUSIONS

The results should illustrate the limitations of modeling due to the inability to preserve all the significant dimensionless groups. This handicap will always be present in fire problems due to the constraint of the physical and chemical processes as well as the constraint imposed by material properties. These difficulties will likely increase with the complexity of the problem studied.

Apparent in this study were several troublesome points. There was an ambiguity in selecting the burning rate in the model since  $\pi_4$  or  $\pi_4'$  could have been used. Moreover the effective heat of combustion of solid fuels burned in fire experiments may not be equal to their theoretical values due to incomplete combustion. Also the radiation dimensionless groups  $\pi_7$  and  $\pi_8$  had to be ignored which resulted in unfavorable, but consistent, results for ceiling temperature and floor irradiance. However, by analysis, it was demonstrated that correlation of floor irradiance could be achieved. Distortion of flame lengths were anticipated and contributed to good agreement for floor heat flux  $H_2$  in the five crib case. This is one example of "good" agreement achieved by compensating effects associated with lack of preservation in flame length and radiation.

In general, the gas-phase convective results for temperature, velocity, and heat transfer coefficient were good as anticipated. In fact the corridor thermal and velocity fields have been studied very extensively in the model by McCaffrey and Quintiere (15,16) under various experimental conditions with good correlation to full-scale behavior. An example from this work (16) is shown in Figure 13 for corridor mid-plane vertical temperature and velocity distribution under nearly geometric and energy input similarity conditions. The flow reversals in the corridor were found to result from the restriction of the corridor exit, and were also observed for the model configuration given in Figure 1.

Finally, the correlation for heat transfer coefficient given in Figure 11 appears to have merit despite the way in which it was derived. A more careful investigation under steady state conditions with correction for radiative heating should improve



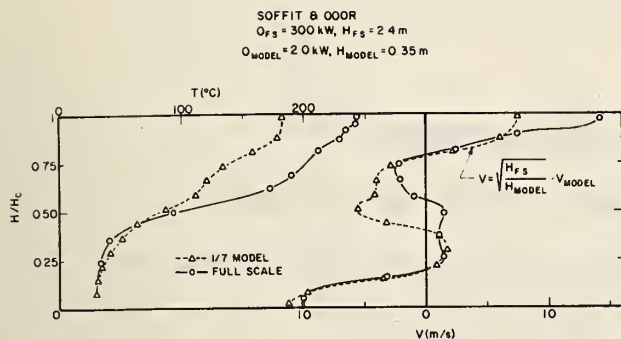


Fig. 13 A comparison of corridor vertical temperature and velocity profiles between model and full-scale under approximate similarity conditions (16).

the accuracy of the results and perhaps decrease the heat transfer coefficient (by about 30 per cent at most).

It would be useful if actual floor covering fire spread could be simulated in the model since this was the subject of the original full-scale experiments (11). Although this may be possible, the design of such model experiments would be subject to assumptions, and the accuracy and interpretation of results would be subject to uncertainties. The results of the relatively simpler experiment modeled here should convey the difficulties of attempting to model the corridor flame spread problem.

From the results of this study it may be concluded that:

1. convective processes associated with fires in enclosures can be scaled successfully;
2. radiative transport is not scaled successfully but results can be improved through analysis or increasing the size of the model;
3. the accuracy of small-scale fire growth studies will depend on the importance of radiation in the prototype problem and how successful it is modeled.

#### ACKNOWLEDGMENTS

The study could not have been effectively done without the support of several persons. The authors would like to express their appreciation to William Rinkinen, who designed and built many of the components in these experiments, Jim Raines, who operated the data acquisition system, Margaret Harkleroad, who programmed the computer for data retrieval and comparison, and Karen Den Braven who assisted in the model experiments and analysis.

#### REFERENCES

- 1 Williams, F. A., "Scaling Mass Fires," Fire Research Abstract Review, Vol. 11, 1969, pp. 1-23.
- 2 Gross, D. and Robertson, A. F., "Experimental Fires in Enclosures," Tenth Symposium (International) on Combustion, The Combustion Institute, 1965, pp. 931-942.

3 Thomas, P. H., "Some Studies of Building Fires Using Models," in *The Use of Models in Fire Research*, W. G. Berl, ed., National Academy of Science - National Research Council, Washington, D.C., 1961, pp. 150-185.

4 Heskestad, G., "Similarity Relations for the Initial Convective Flow Generated by Fire," ASME paper 72-WA/HT-17, Nov. 1972.

5 Heskestad, G., "Physical Modeling of Fire," J. Fire and Flammability, Vol. 6, 1975, pp. 253-273.

6 Lee, B. T., "Laboratory Scaling of the Fluid Mechanical Aspects of Large Fires," Combustion Science Technology, Vol. 5, 1972, pp. 233-239.

7 Yokoi, S., "Upward Convection Current from a Burning Wooden House," in *The Use of Models in Fire Research*, W. G. Berl, ed., National Academy of Science - National Research Council, Washington, D.C., 1961, pp. 186-218.

8 de Ris, J., Kanury, A. M., and Yuen, M. C., "Pressure Modeling of Fires," Fourteenth Symposium (International) on Combustion, The Combustion Institute, 1973, pp. 1033-1044.

9 Alpert, R. L., "Pressure Modeling Transient Crib Fires," ASME Paper No. 75-HT-6, August 1975.

10 Parker, W. J. and Lee, B. T., "A Small-Scale Enclosure for Characterizing the Fire Buildup Potential in a Room," NBSIR 75-710, National Bureau of Standards, Washington, D.C., June 1975.

11 Quintiere, J., "Some Observations on Building Corridor Fires," Fifteenth Symposium (International) on Combustion, The Combustion Institute, 1974, pp. 163-174.

12 Quintiere, J., "The Application and Interpretation of a Test Method to Determine the Hazard of Floor Covering Fire Spread in Building Corridors," International Symposium: Fire Safety of Combustible Materials, Univ. Edinburgh, Oct. 1975, pp. 355-366a.

13 Steward, F. R., "Prediction of the Height of Turbulent Diffusion Buoyant Flames," Combustion Science Technology, Vol. 2, 1970, pp. 203-212.

14 Kawagoe, K., "Fire Behavior in Rooms," Rep. No. 27, The Building Research Institute, Japan, Sept. 1958.

15 McCaffrey, B. J., and Quintiere, J. G., "Fire-Induced Corridor Flow in a Scale Model Study," Symposium on the Control of Smoke Movement in Building Fires, Proceedings, Conseil International du Bâtiment (CIB), Garston, U.K. Nov. 4-5, 1975, pp. 33-47.

16 McCaffrey, B. J., and Quintiere, J. G., "Buoyancy Driven Countercurrent Flows Generated by a Fire Source," *Turbulent Buoyant Convection*, Hemisphere Publ. Corp., (to be published), pp. 457-472.

### COMPLETE SET OF SCALING RESULTS

The complete set of scaling results follow and supplement Figures 3 - 8 of the previous section. Also Figure 1 is repeated at a larger size for clarity.

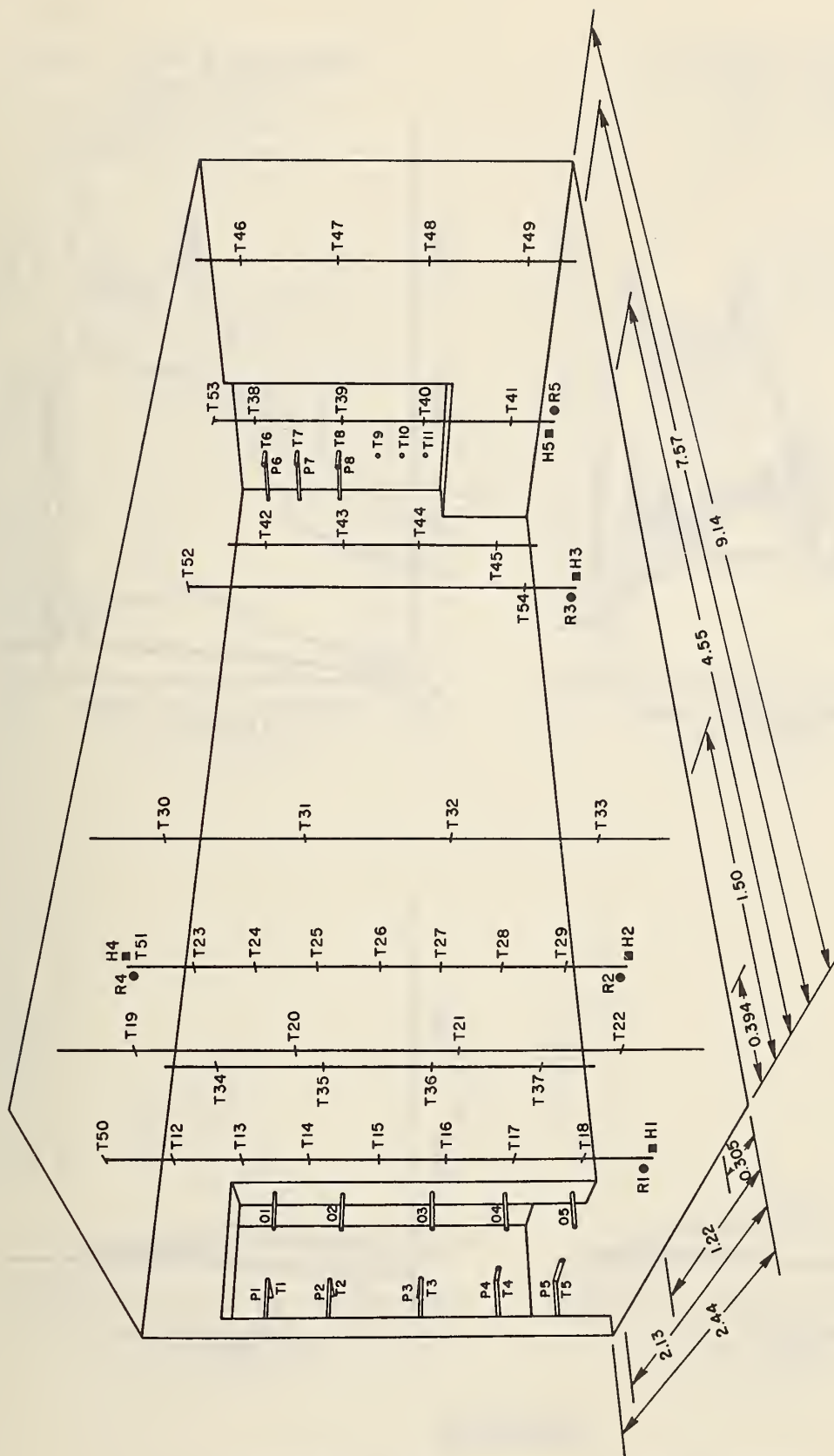


Figure 1. Corridor geometry and instrumentation for the full-scale experiments (distance in meters)

CORRIDOR FIRE - 1 CRIB  
ROOM DOORWAY

— FULL SCALE  
— 1/7 SCALE

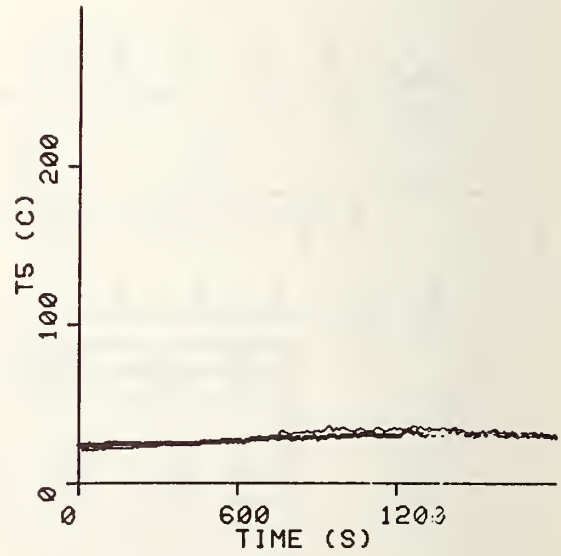
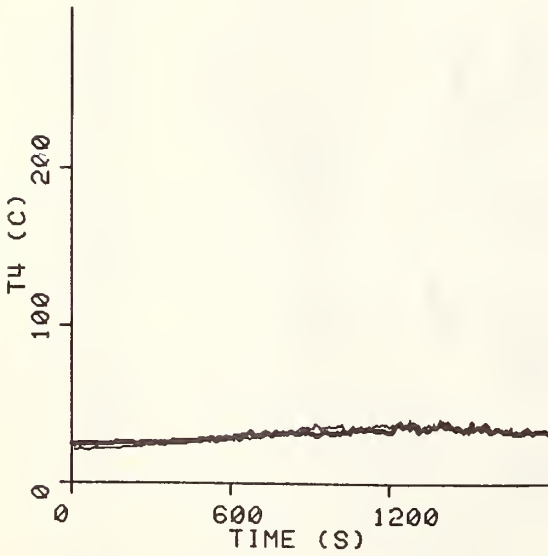
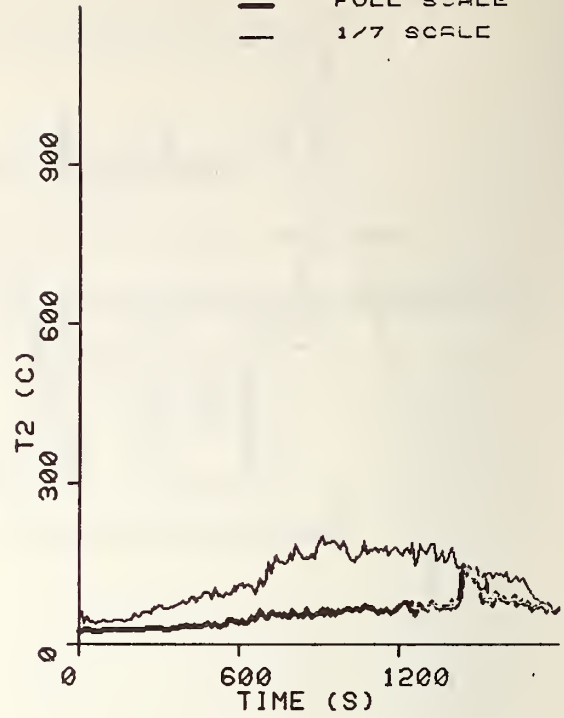
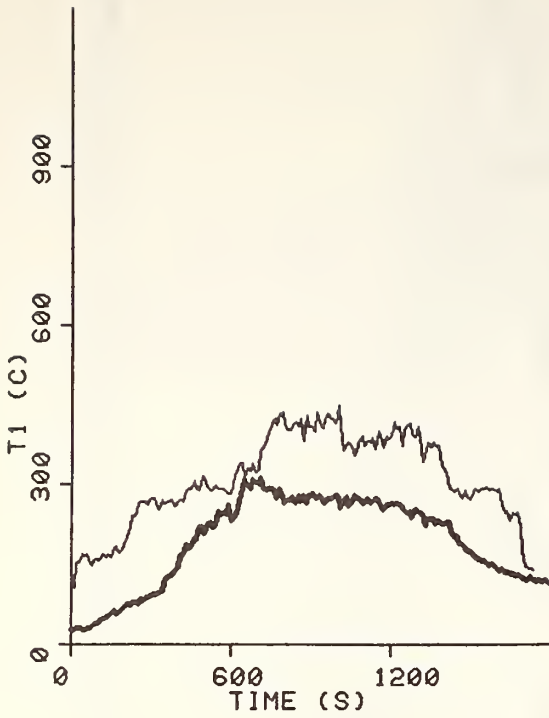


Figure 14a

Figures 14a-e: TEMPERATURES AT ROOM DOORWAY

CORRIDOR FIRE - 2 CRIBS  
ROOM DOORWAY

— FULL SCALE  
— 1/7 SCALE

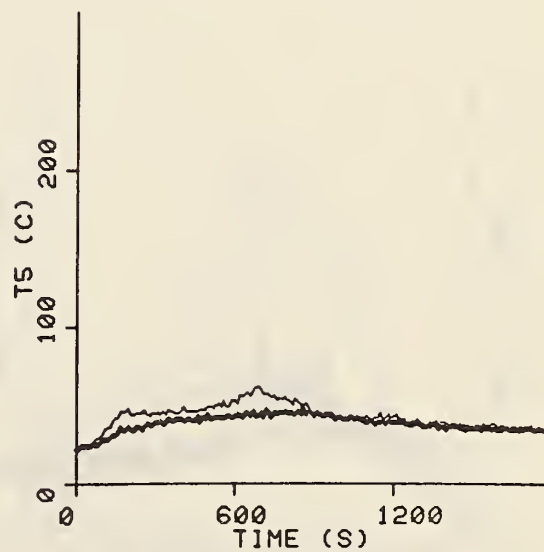
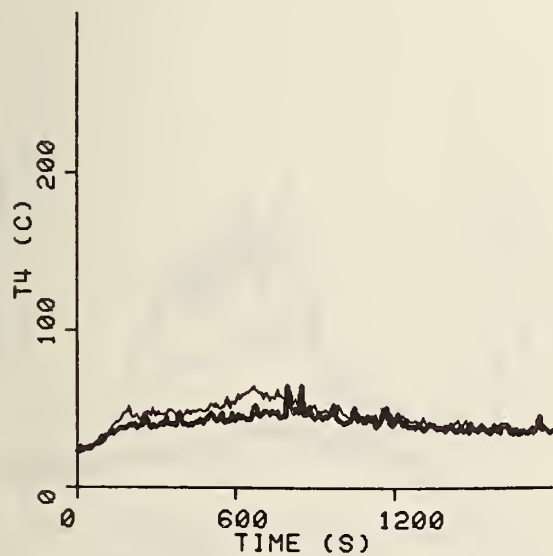
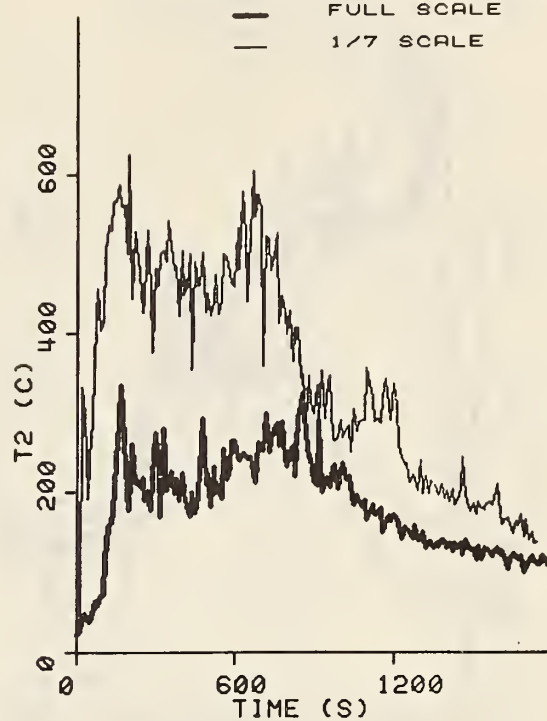


Figure 14b



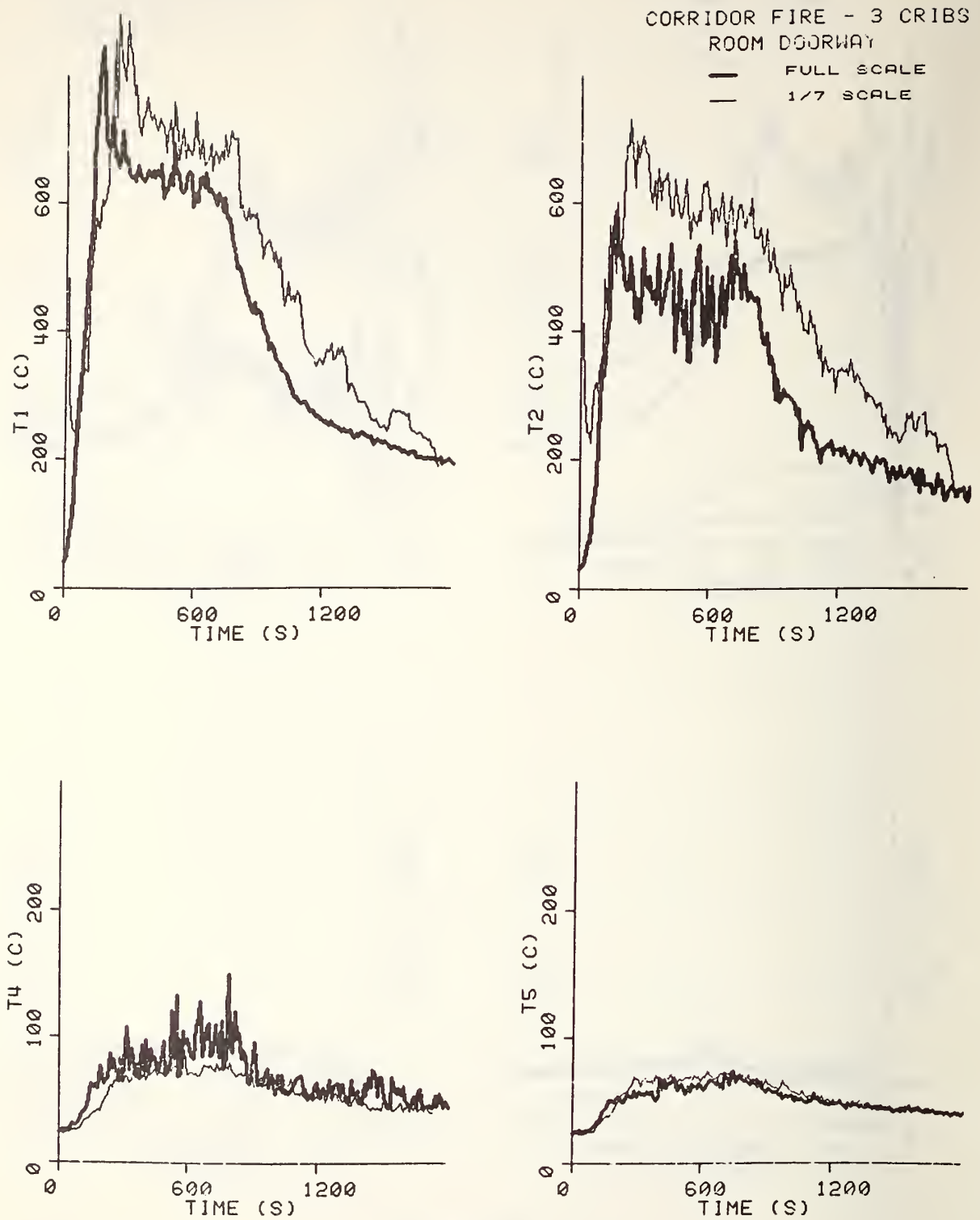


Figure 14c

CORRIDOR FIRE - 4 CRIBS  
ROOM DOORWAY

— FULL SCALE  
— 1/7 SCALE

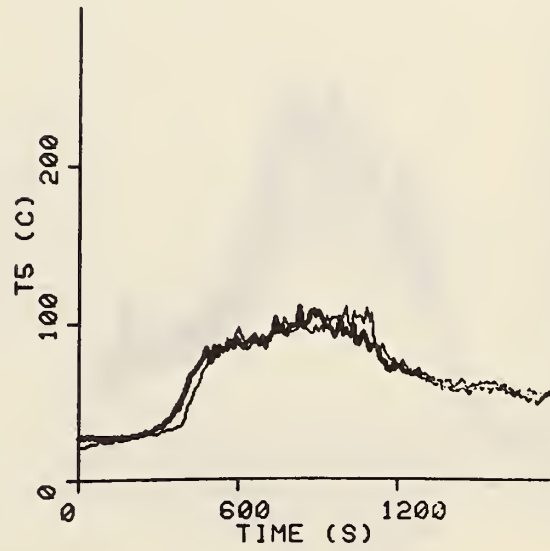
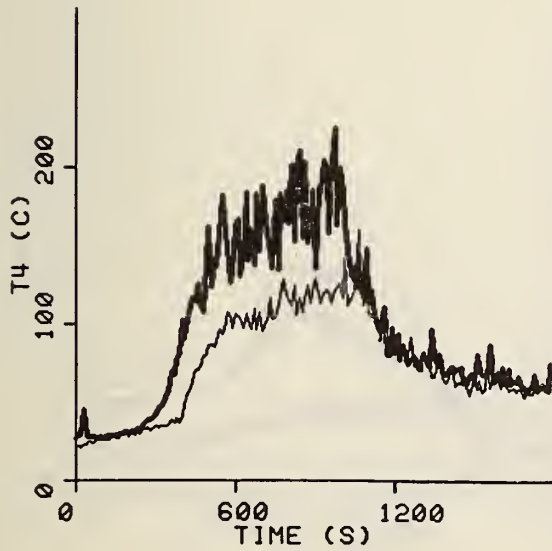
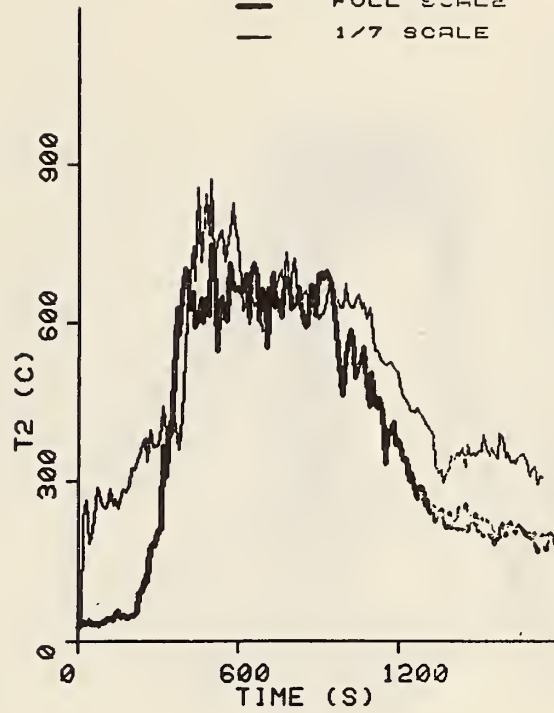
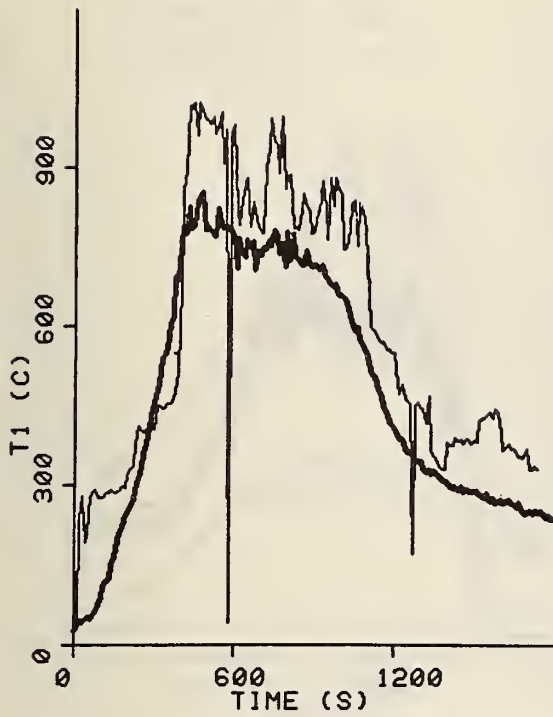


Figure 14d

CORRIDOR FIRE - 5 CRIBS  
ROOM DOORWAY

— FULL SCALE  
— 1/7 SCALE

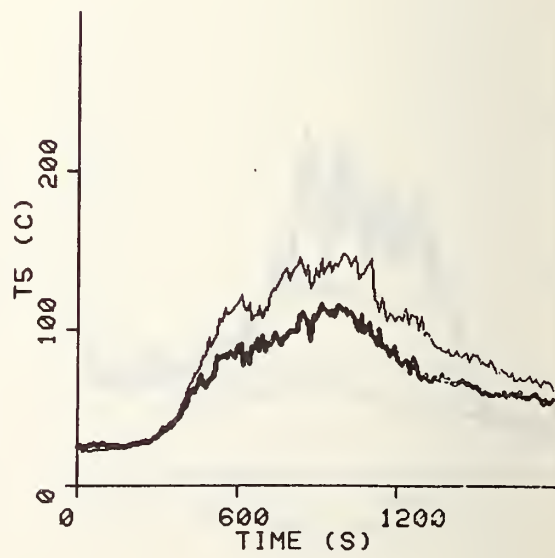
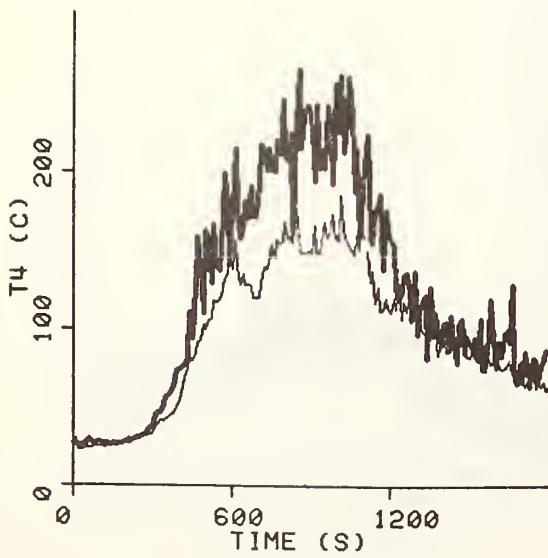
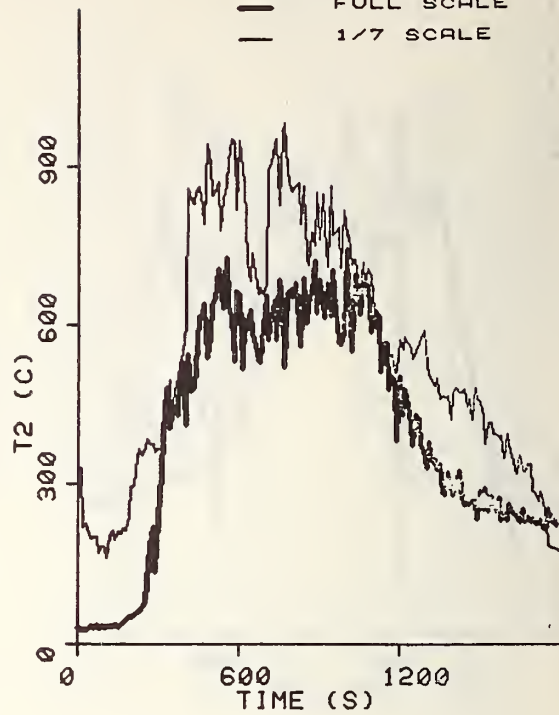
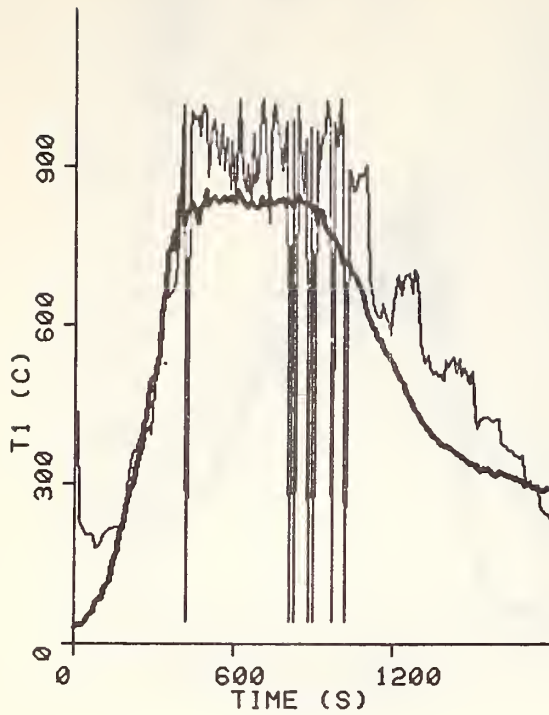


Figure 14e



CORRIDOR FIRE - 1 CRIB  
5 FT. CORRIDOR

— FULL SCALE  
— 1/7 SCALE

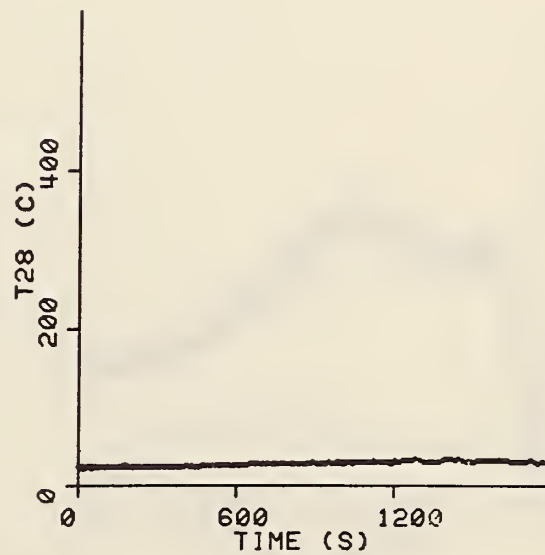
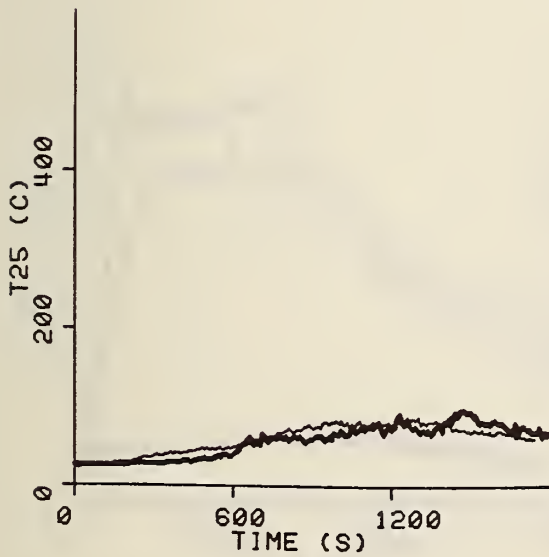
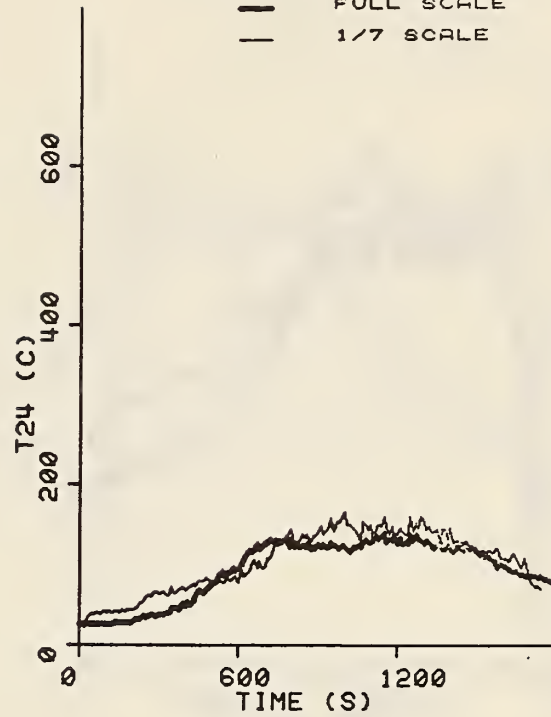
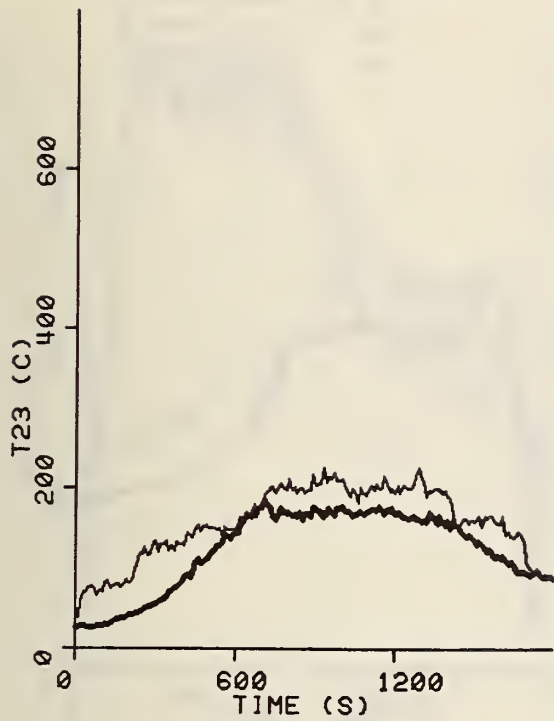


Figure 15a

Figures 15a-e: TEMPERATURES IN CORRIDOR AT 1.5 m (5 ft) from rear wall

CORRIDOR FIRE - 2 CRIBS  
5 FT. CORRIDOR

— FULL SCALE  
— 1/7 SCALE

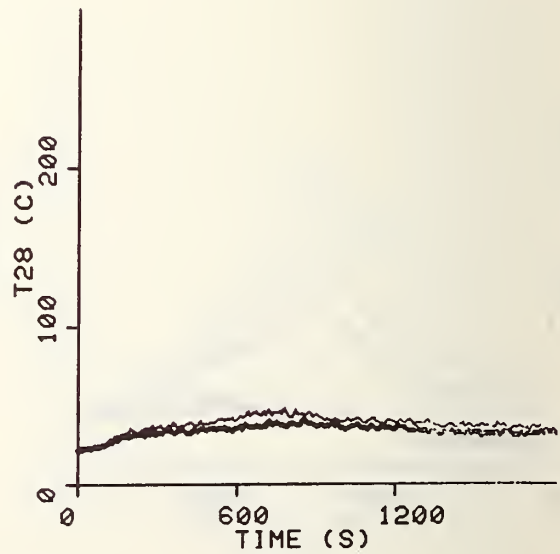
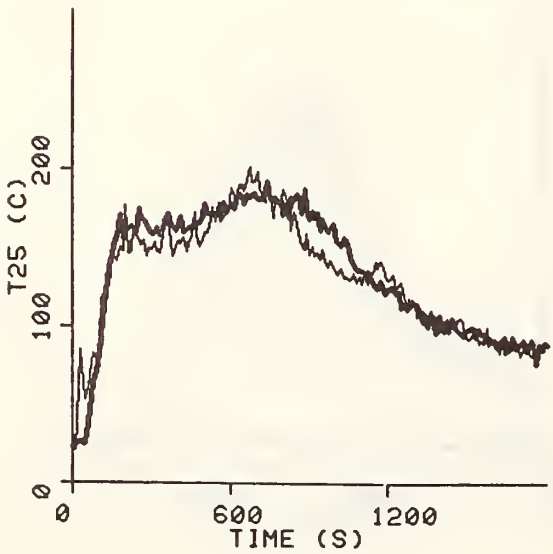
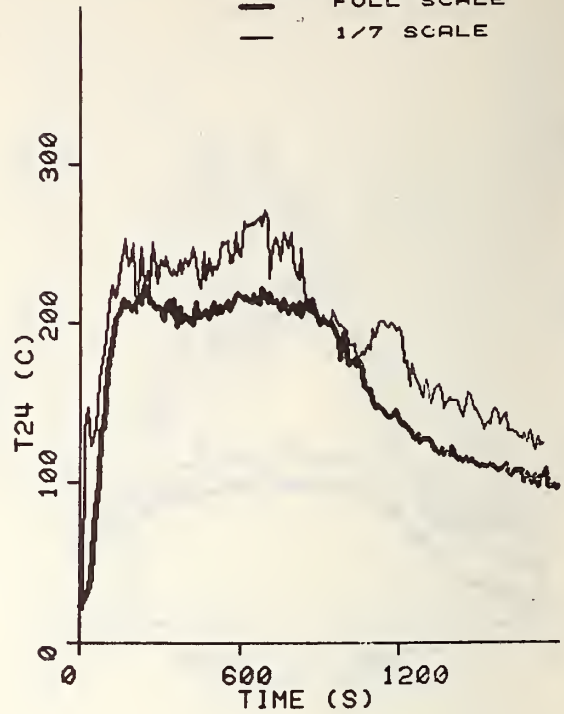


Figure 15b

CORRIDOR FIRE - 3 CRIBS

5 FT. CORRIDOR

— FULL SCALE

— 1/7 SCALE

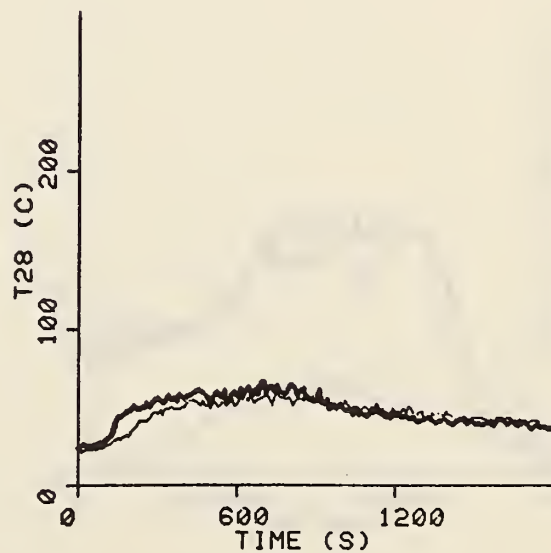
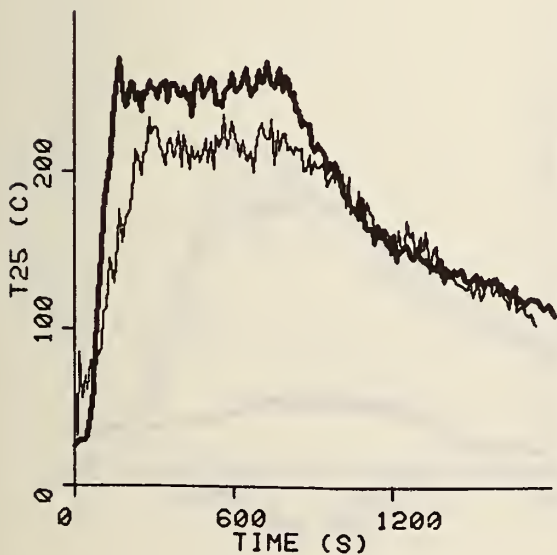


Figure 15c

CORRIDOR FIRE - 4 CRIBS  
5 FT. CORRIDOR

— FULL SCALE  
— 1/7 SCALE

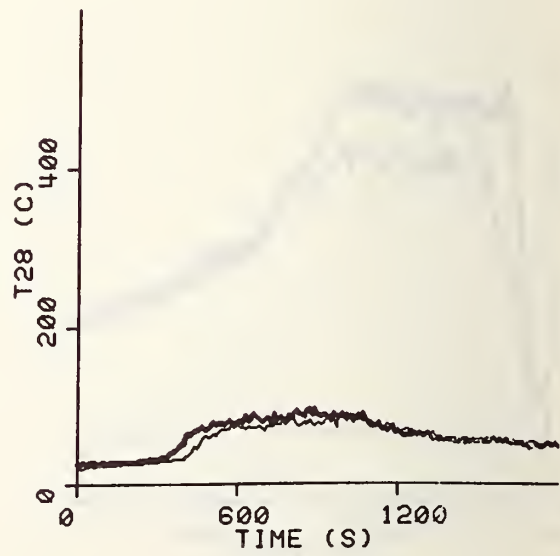
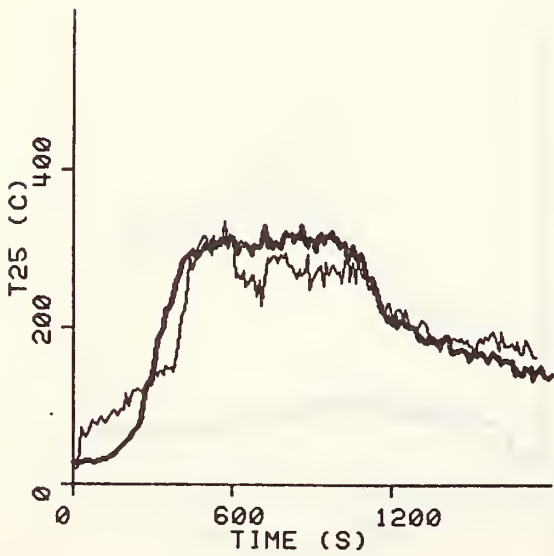
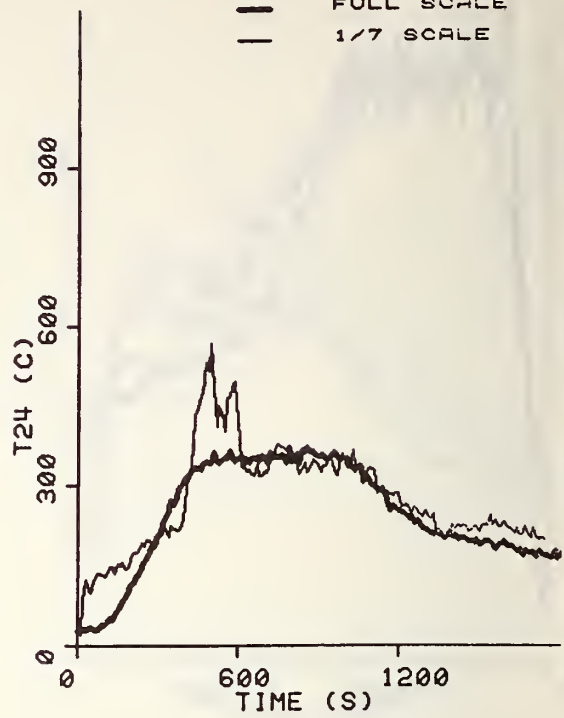
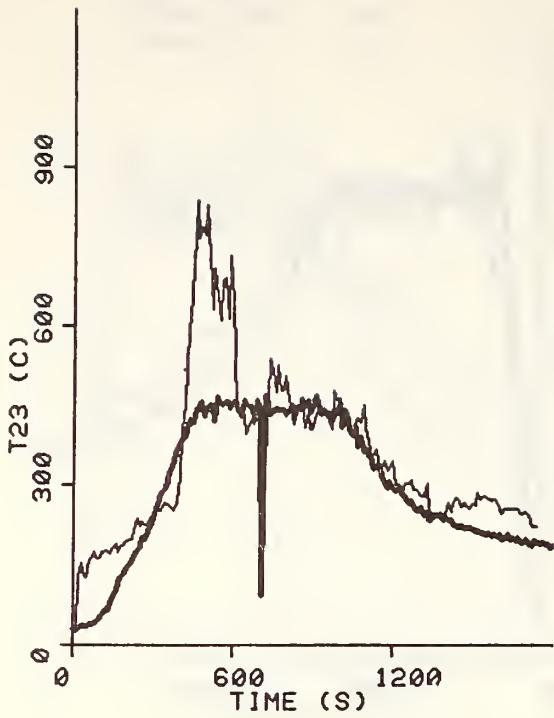


Figure 15d

CORRIDOR FIRE - 5 CRIBS  
5 FT. CORRIDOR

— FULL SCALE  
— 1/7 SCALE

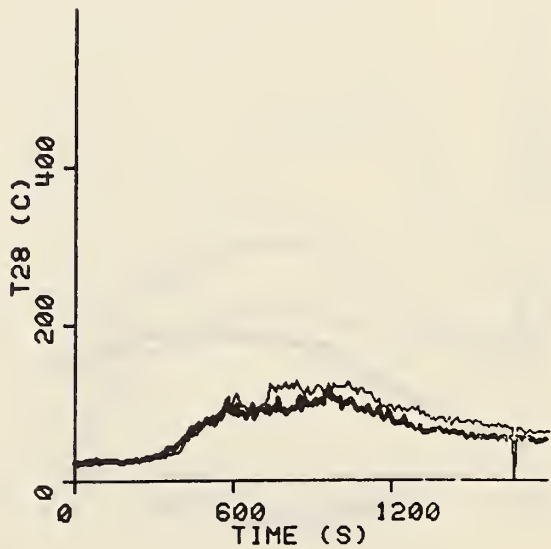
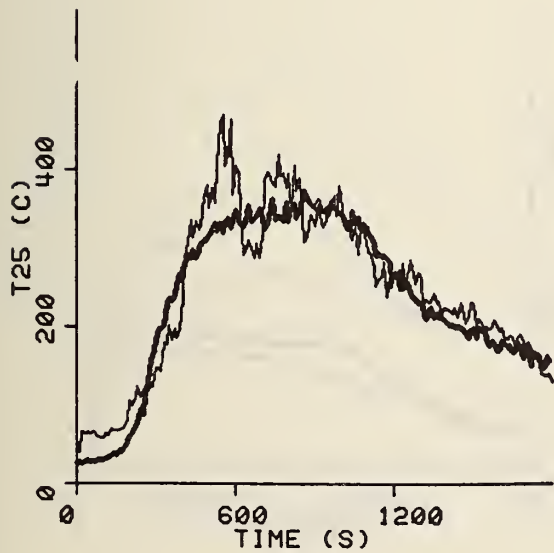
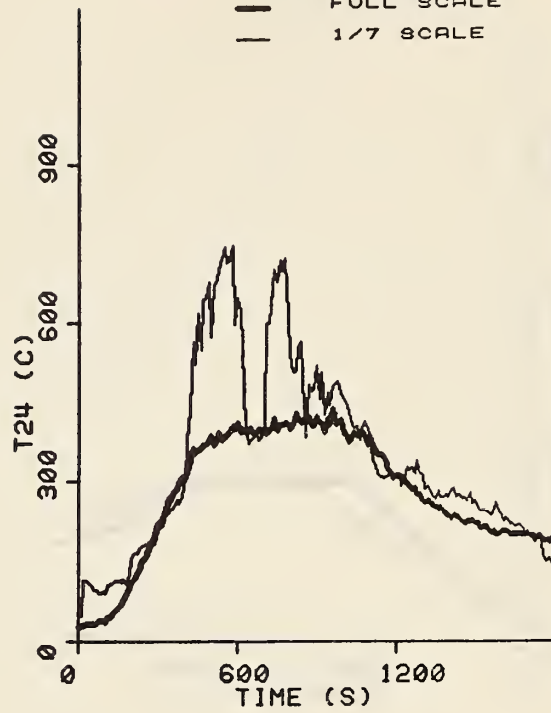
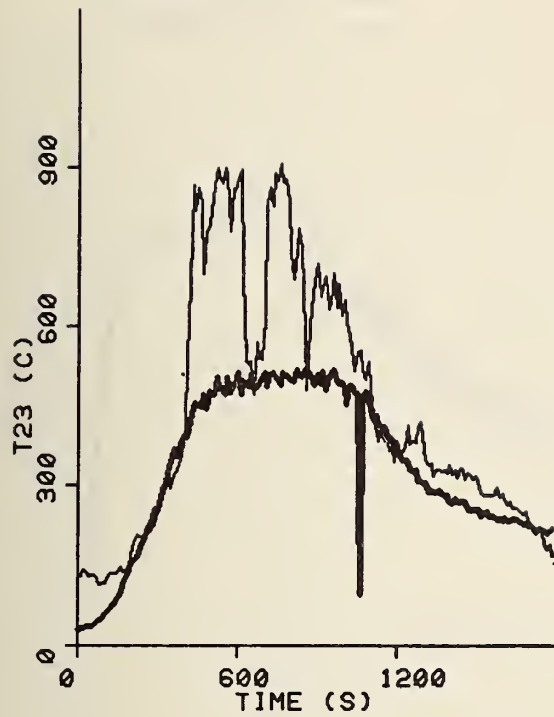


Figure 15e

CORRIDOR FIRE - 1 CRIB  
CEILING

— FULL SCALE  
— 1/7 SCALE

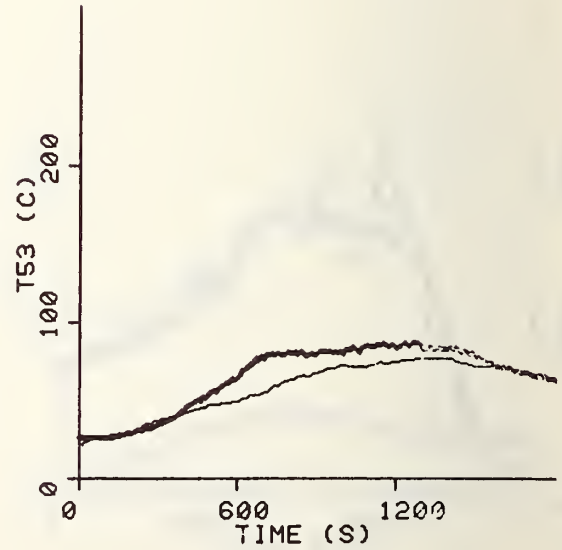
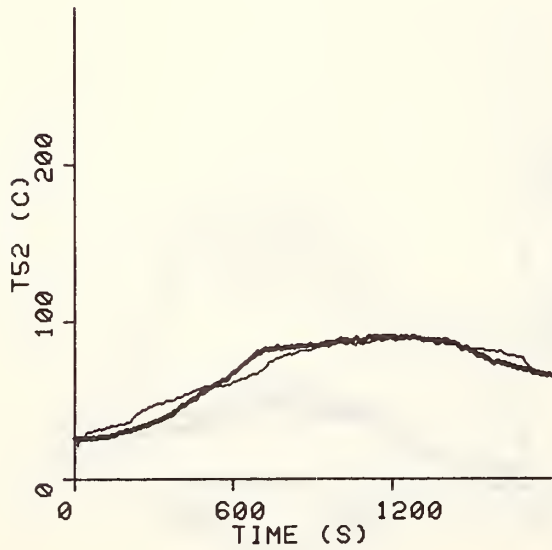


Figure 16a

Figures 16a-e: CORRIDOR CEILING TEMPERATURES



CORRIDOR FIRE - 2 CRIBS  
CEILING

— FULL SCALE  
— 1/7 SCALE

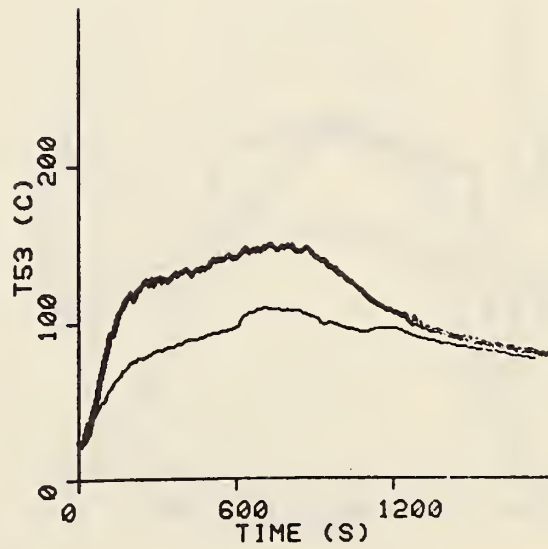
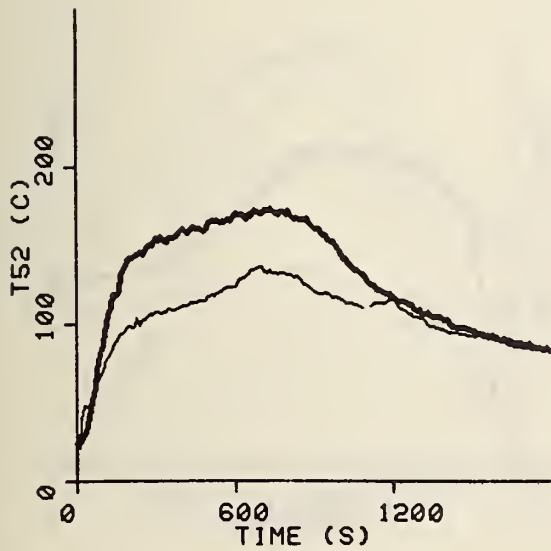
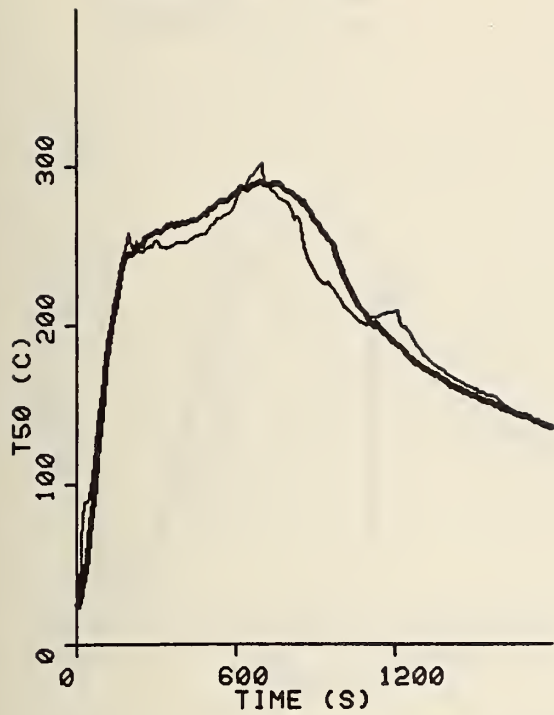


Figure 16b  
27

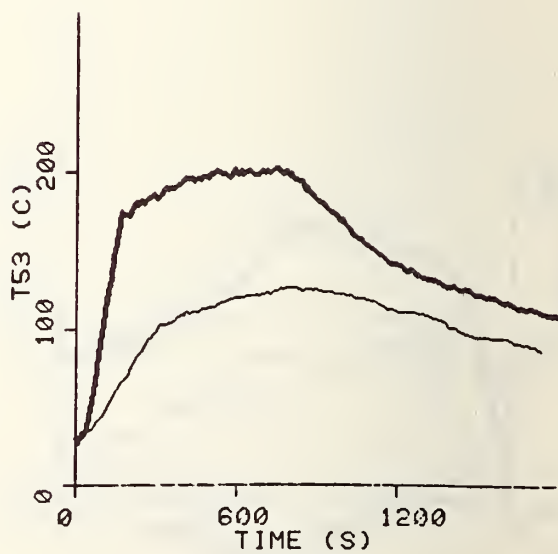
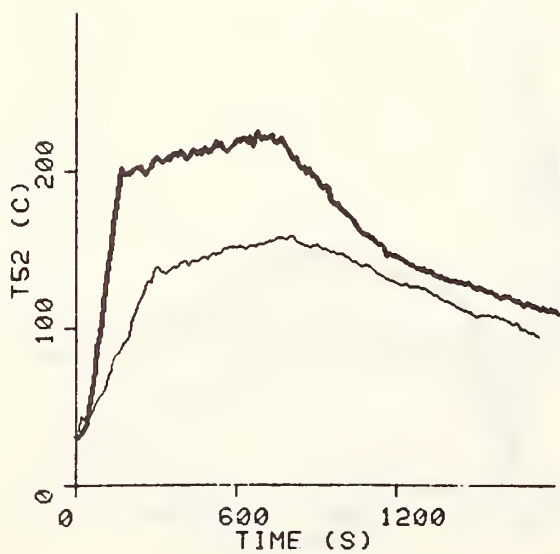
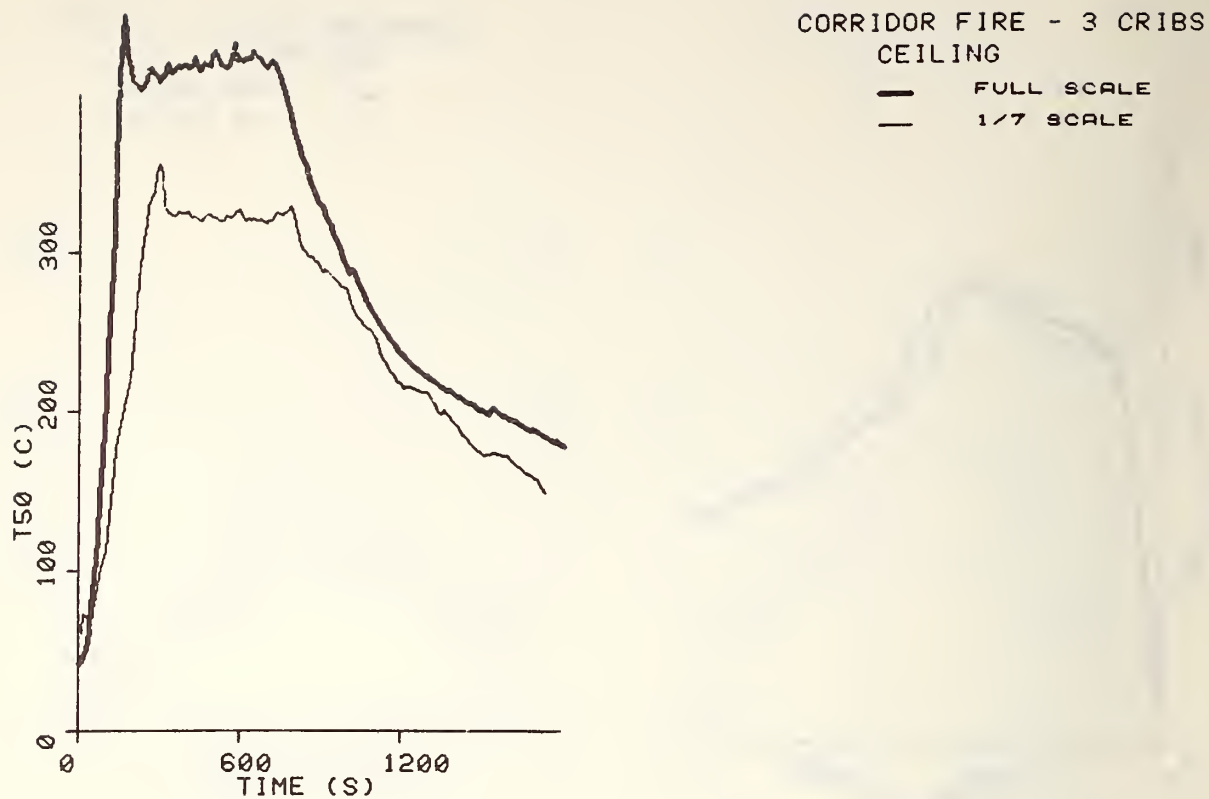


Figure 16c  
28



CORRIDOR FIRE - 4 CRIBS  
CEILING

— FULL SCALE  
— 1/7 SCALE

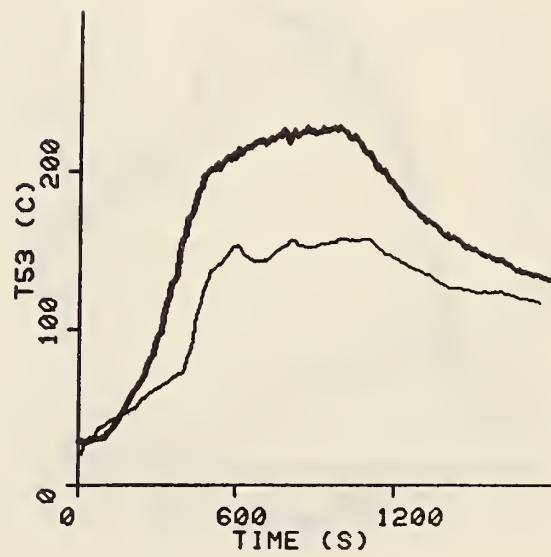
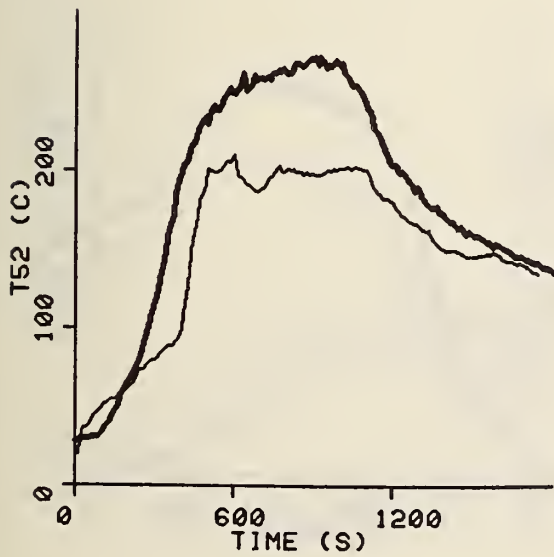
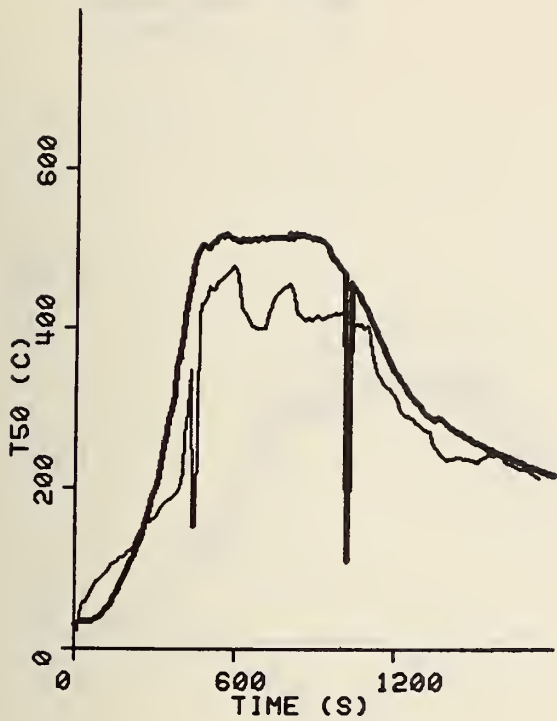


Figure 16d

CORRIDOR FIRE - 5 CRIBS  
CEILING

— FULL SCALE  
— 1/7 SCALE

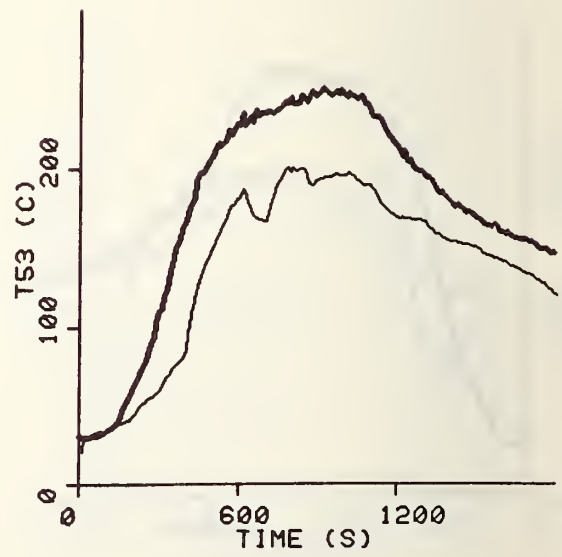
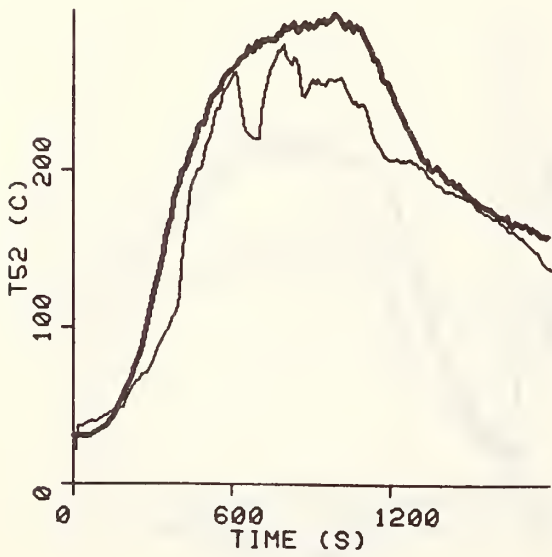
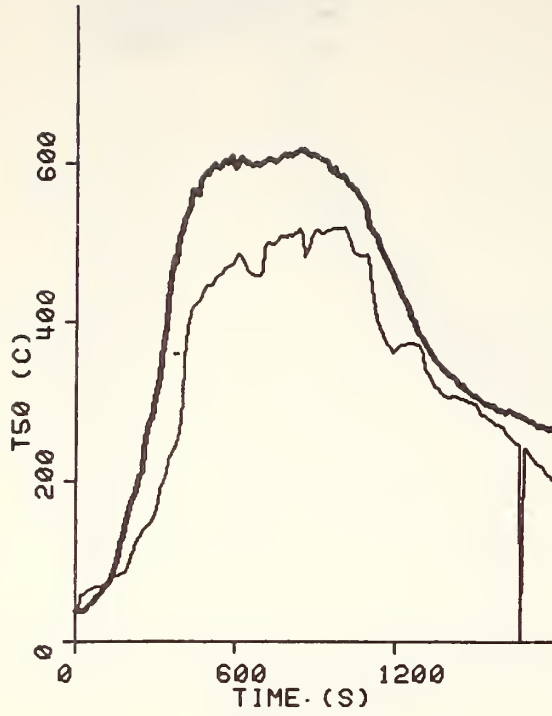


Figure 16e

CORRIDOR FIRE - 1 CRIB  
RADIATION

— FULL SCALE  
— 1/7 SCALE

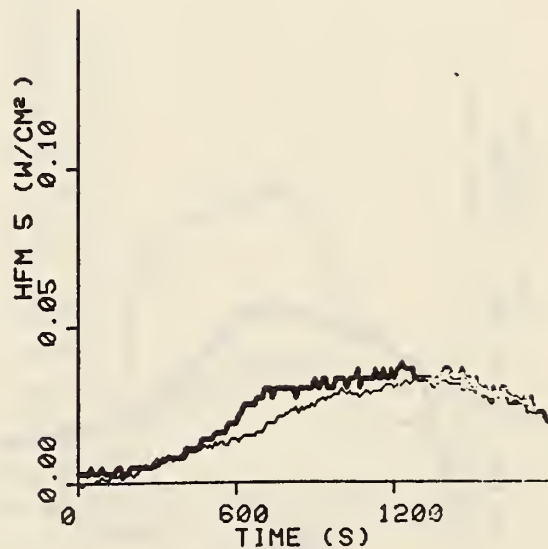
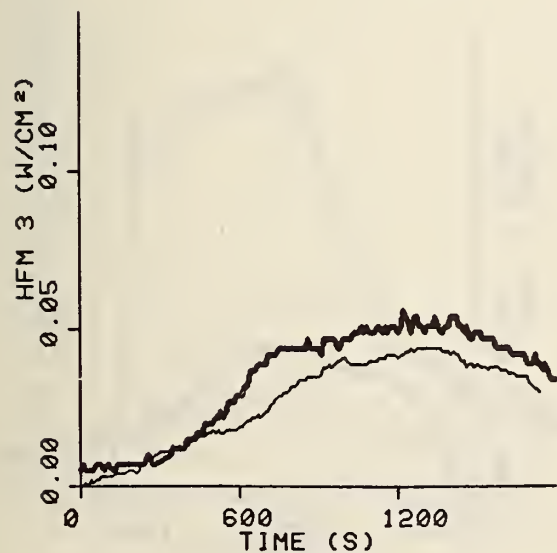
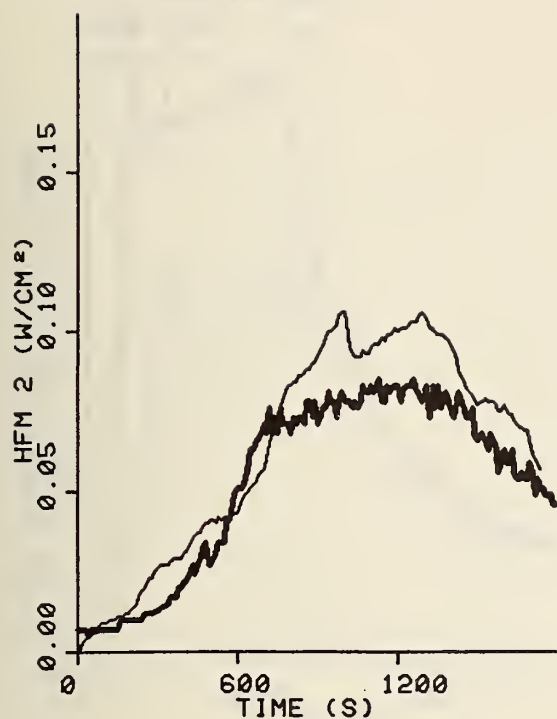


Figure 17a

Figures 17a-e: INCIDENT RADIATION TO CORRIDOR FLOOR

CORRIDOR FIRE - 2 CRIBS  
RADIATION

— FULL SCALE  
— 1/7 SCALE

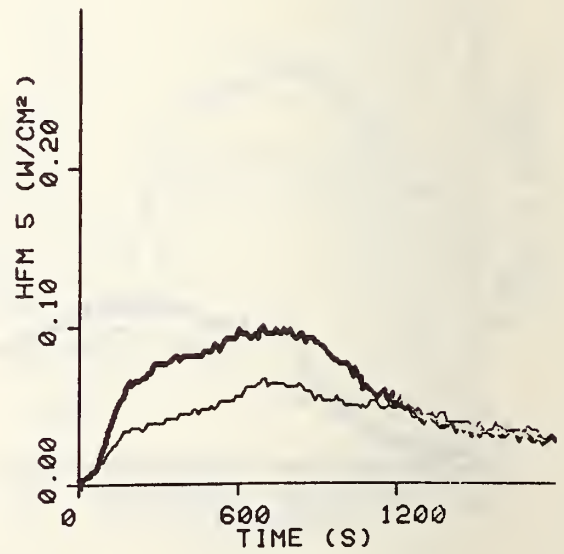
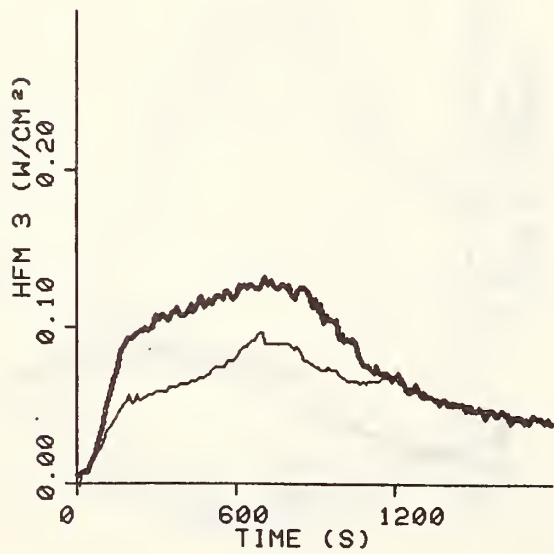


Figure 17b

CORRIDOR FIRE - 3 CRIBS  
RADIATION

— FULL SCALE  
— 1/7 SCALE

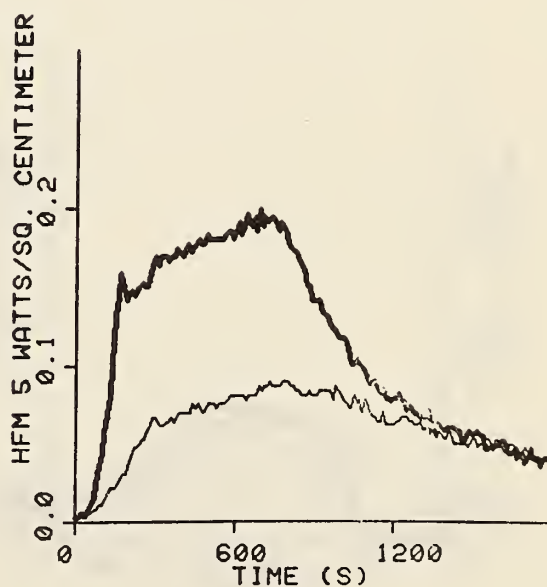
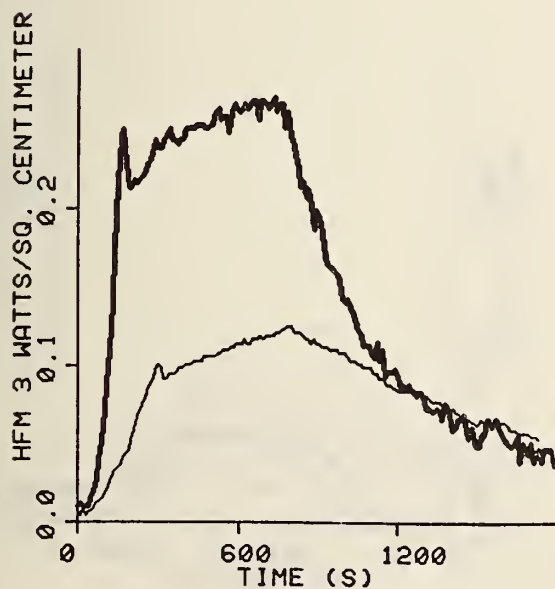


Figure 17c

CORRIDOR FIRE - 4 CRIBS  
RADIATION

— FULL SCALE  
— 1/7 SCALE

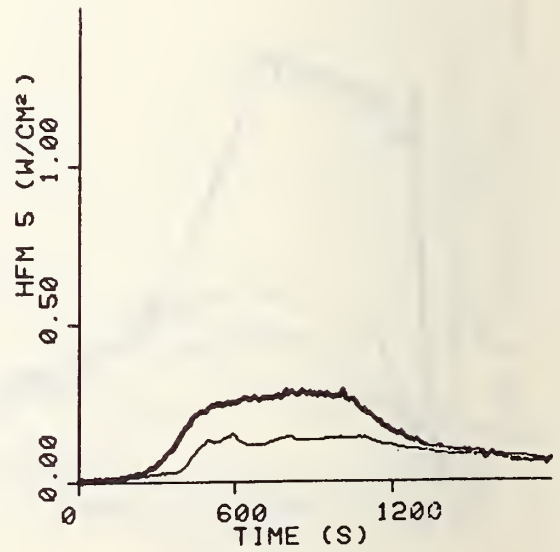
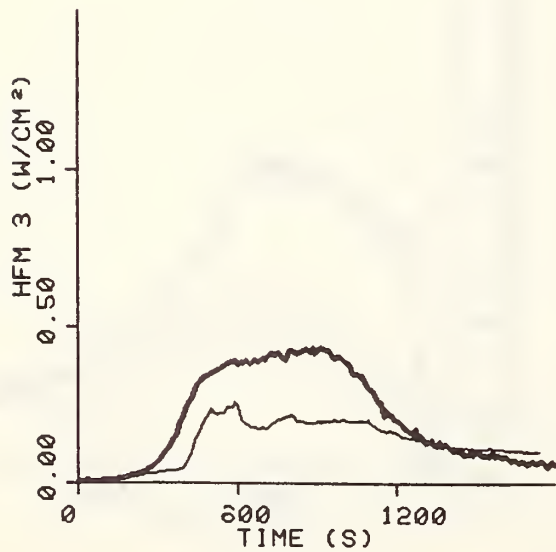
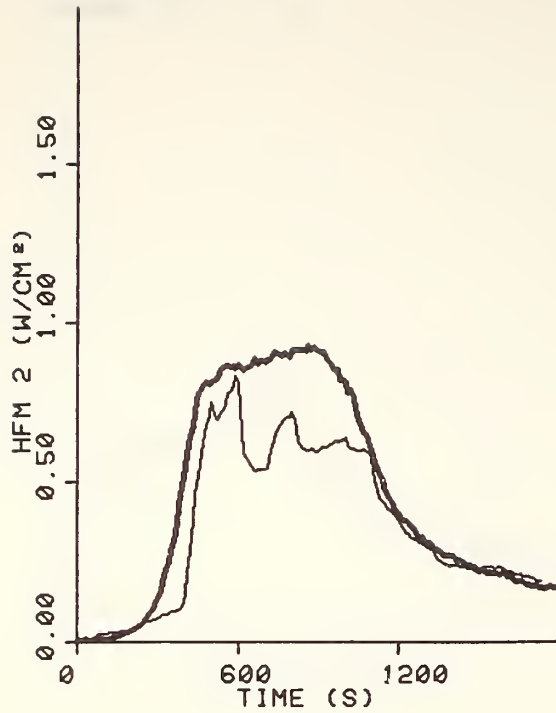


Figure 17d



CORRIDOR FIRE - 5 CRIBS  
RADIATION

— FULL SCALE  
— 1/7 SCALE

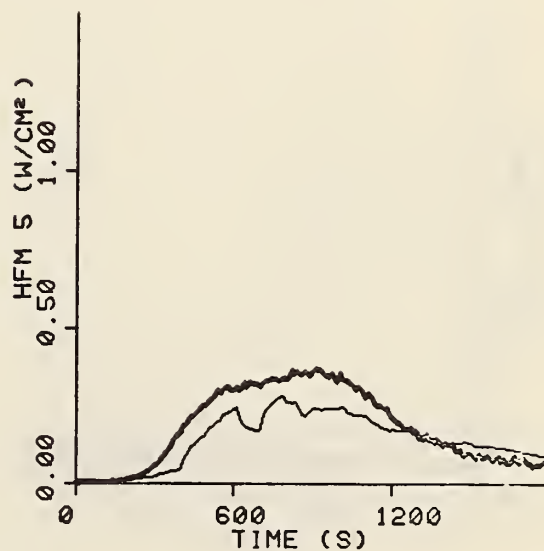
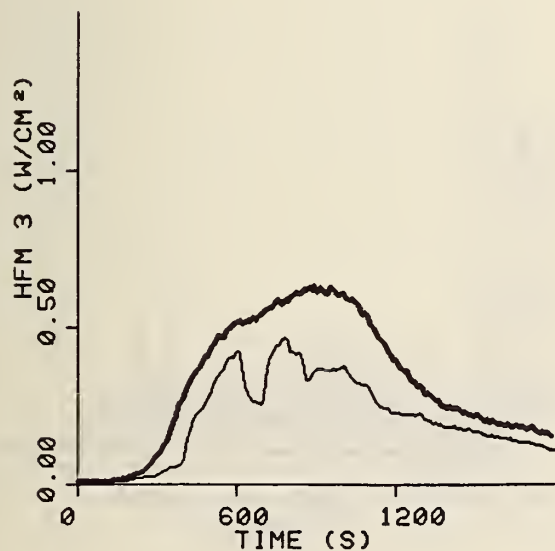
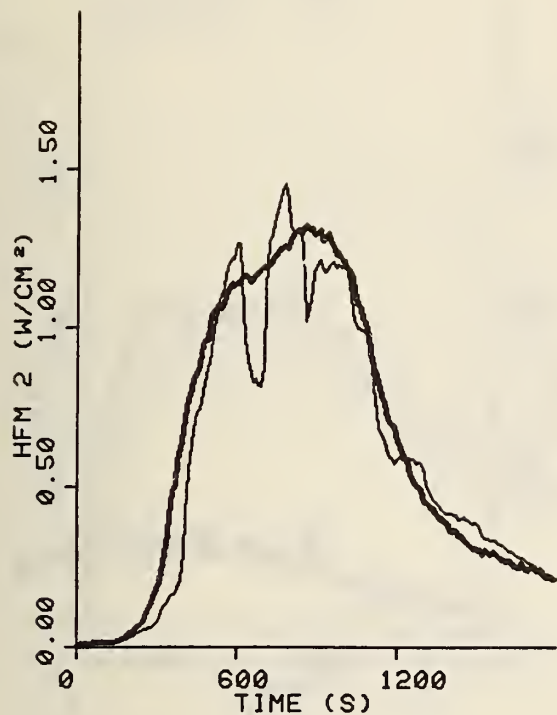


Figure 17e

CORRIDOR FIRE - 1 CRIB  
EXIT WINDOW

— FULL SCALE  
— 1/7 SCALE

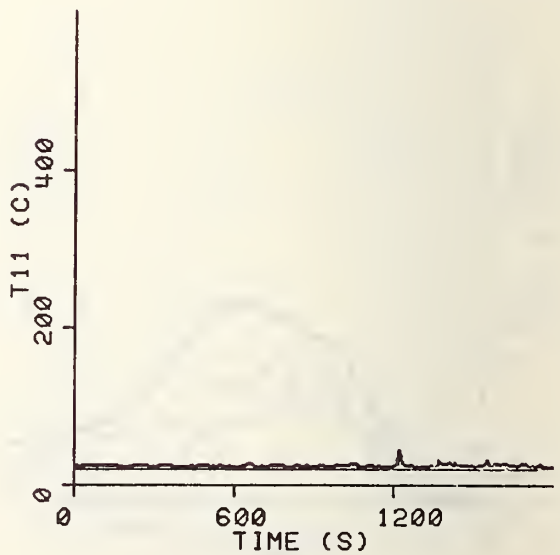
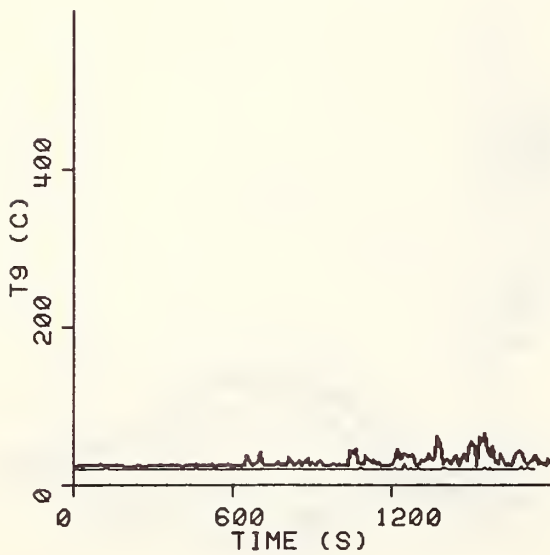
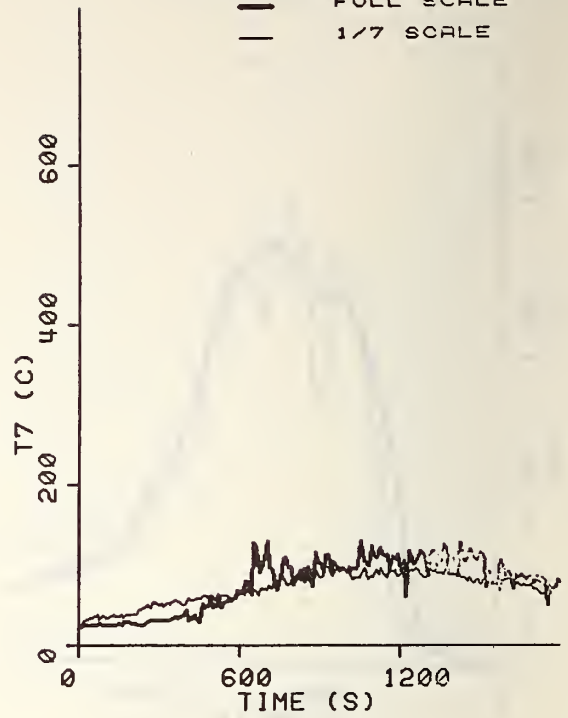
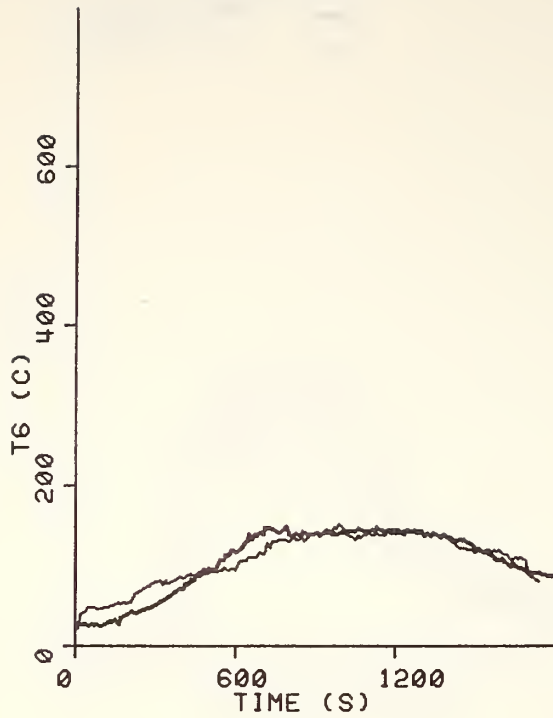


Figure 18a

Figures 18a-e: TEMPERATURES AT THE CORRIDOR EXIT WINDOW

CORRIDOR FIRE - 2 CRIBS  
EXIT WINDOW

— FULL SCALE  
— 1/7 SCALE

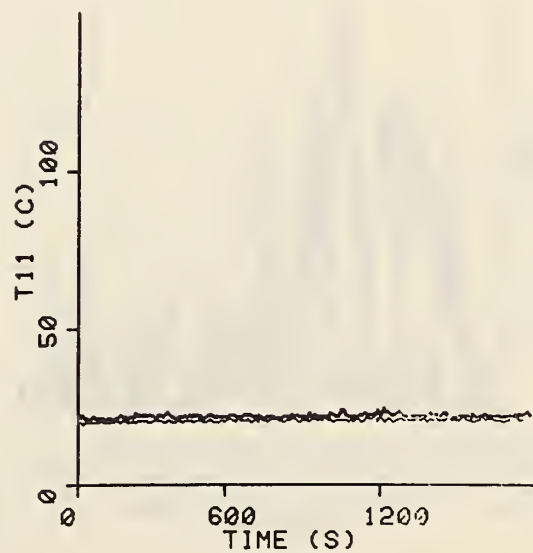
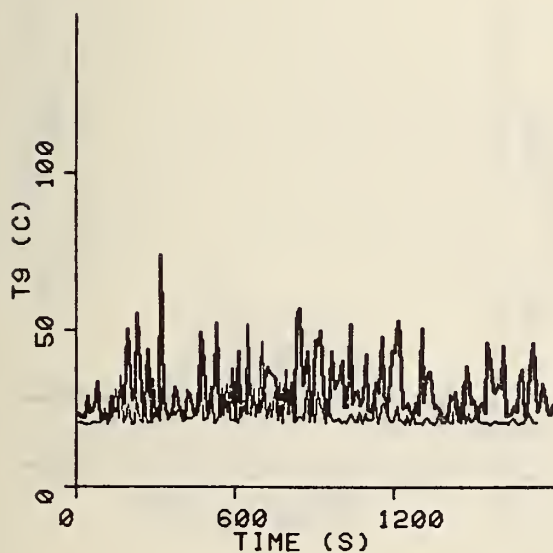


Figure 18b

CORRIDOR FIRE - 3 CRIBS  
EXIT WINDOW

— FULL SCALE  
— 1/7 SCALE

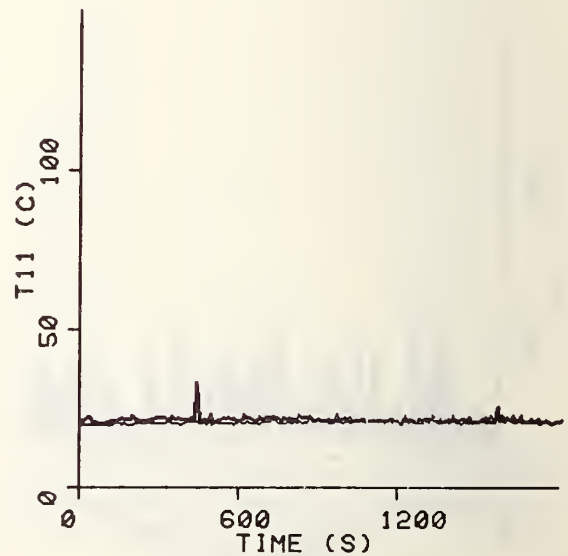
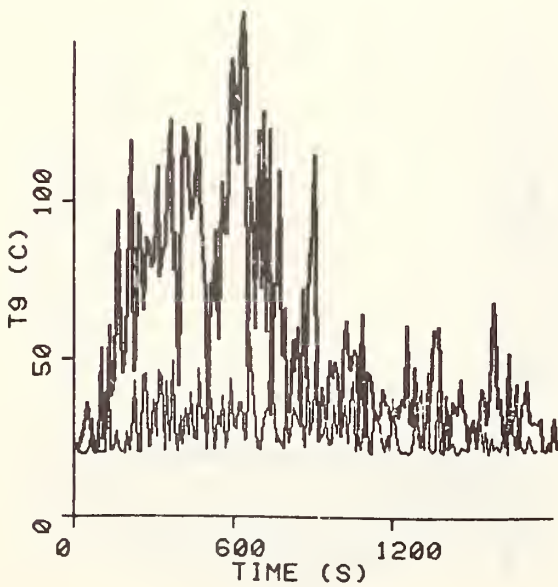
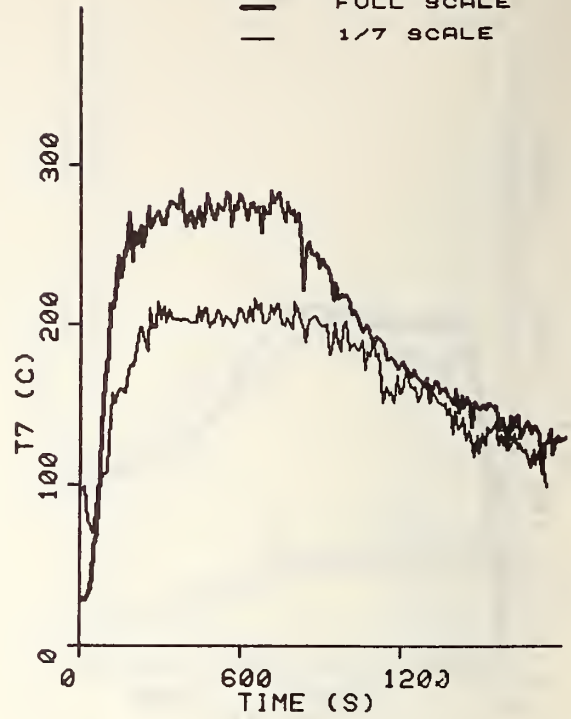


Figure 18c

CORRIDOR FIRE - 4 CRIBS  
EXIT WINDOW

— FULL SCALE  
— 1/7 SCALE

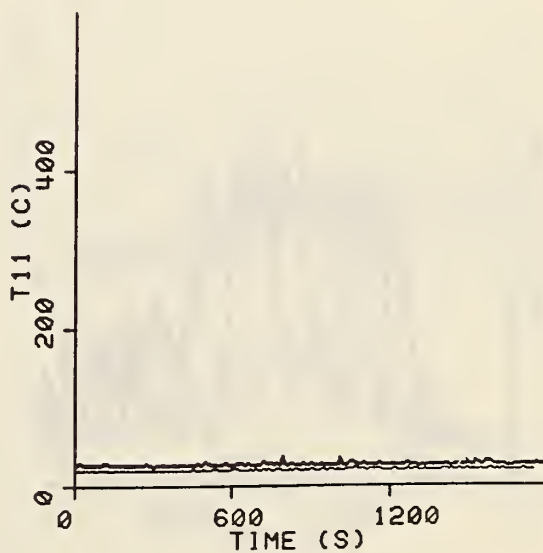
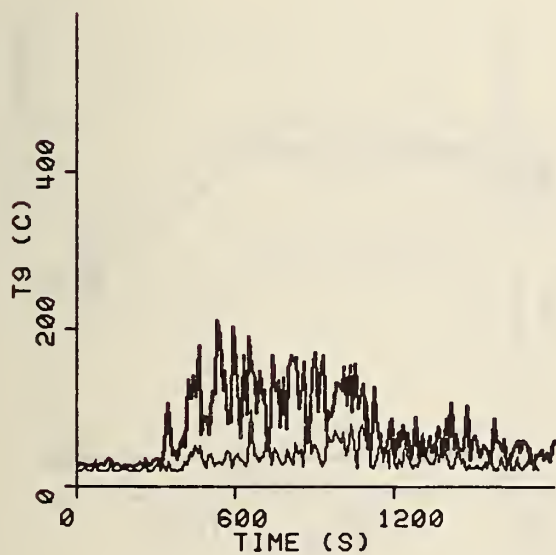
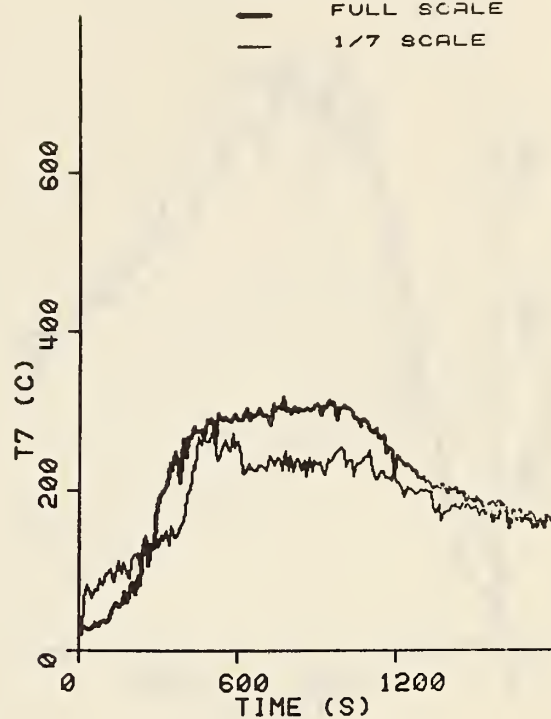
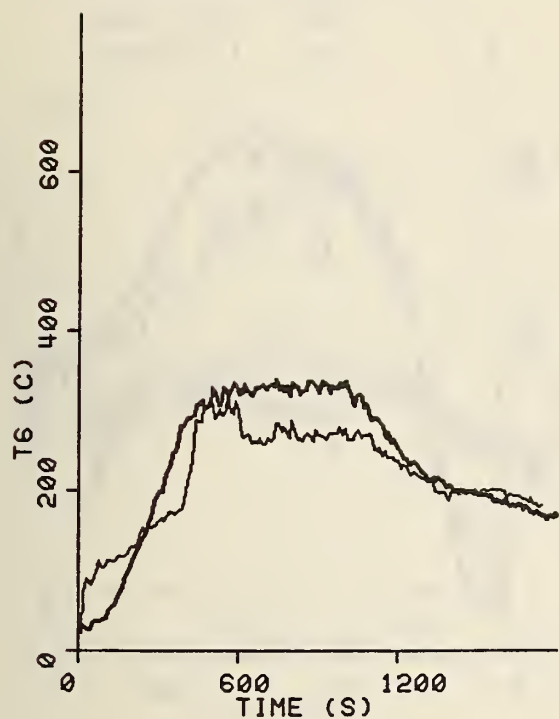


Figure 18d



CORRIDOR FIRE - 5 CRIBS  
EXIT WINDOW

— FULL SCALE  
— 1/7 SCALE

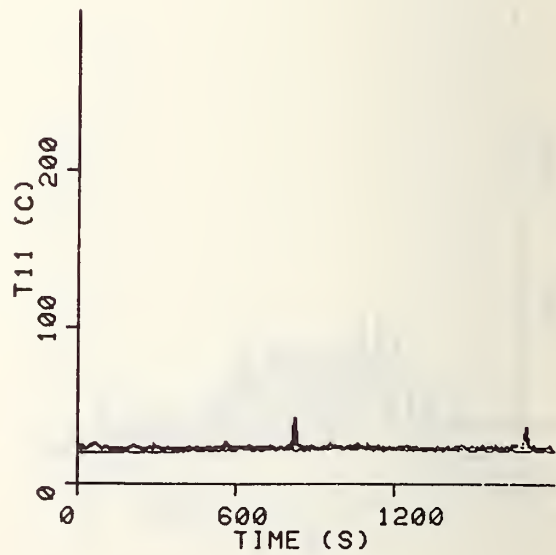
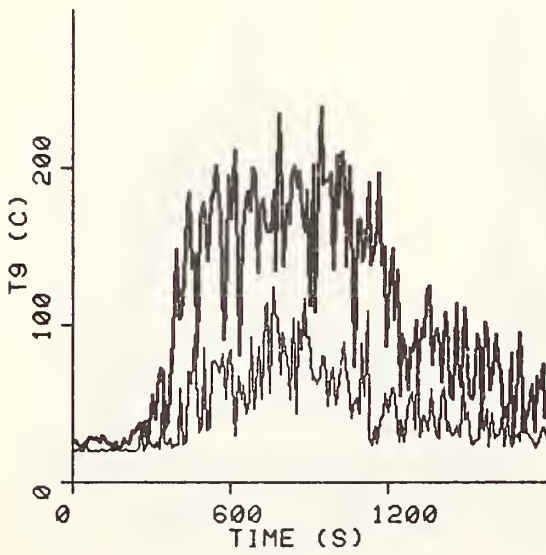
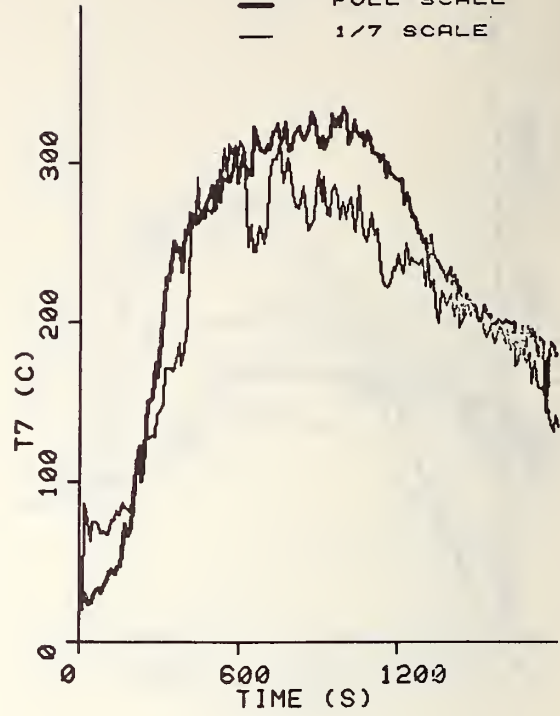
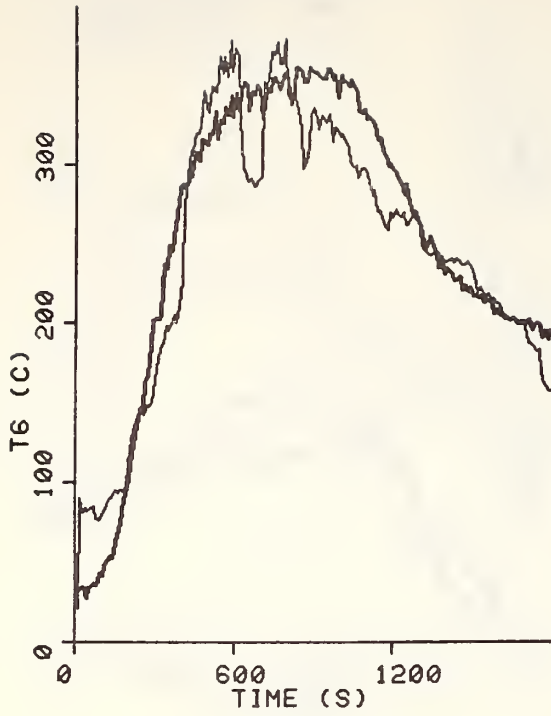


Figure 18e

CORRIDOR FIRE - 1 CRIB  
HEAT TRANSFER COEFFICIENT  
VELOCITY

— FULL SCALE  
— 1/7 SCALE

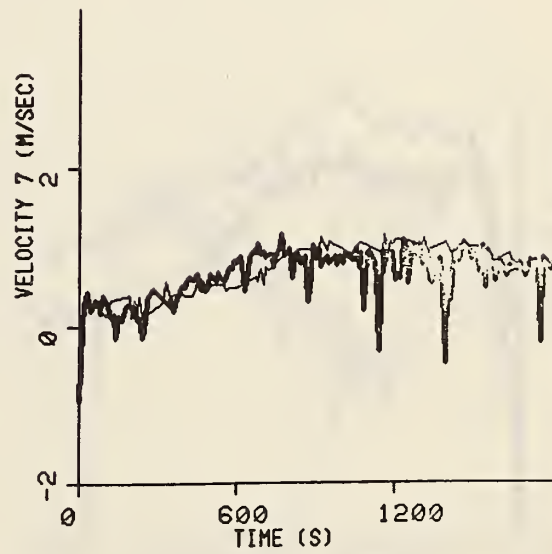
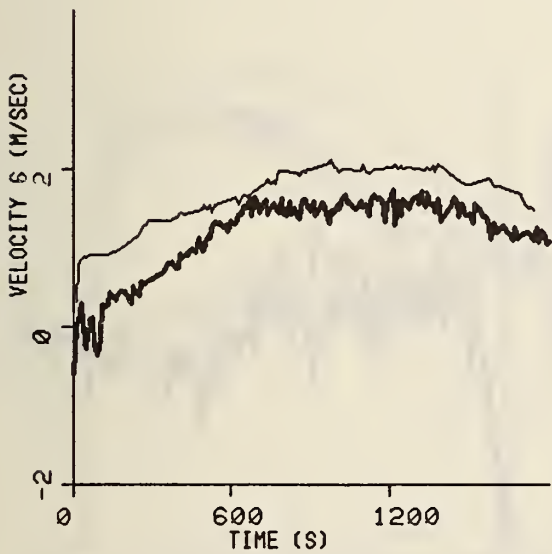
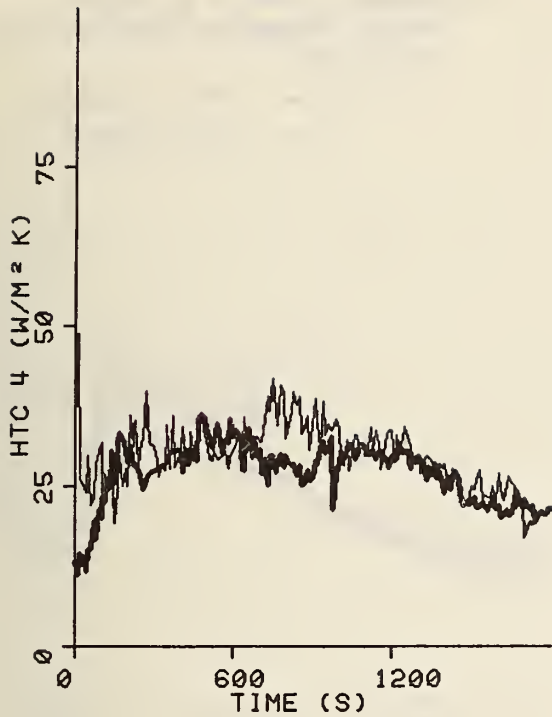


Figure 19a

Figures 19a-e: CEILING HEAT TRANSFER COEFFICIENT  
AND  
EXIT WINDOW VELOCITIES

CORRIDOR FIRE - 2 CRIBS  
HEAT TRANSFER COEFFICIENT  
VELOCITY

— FULL SCALE  
— 1/7 SCALE

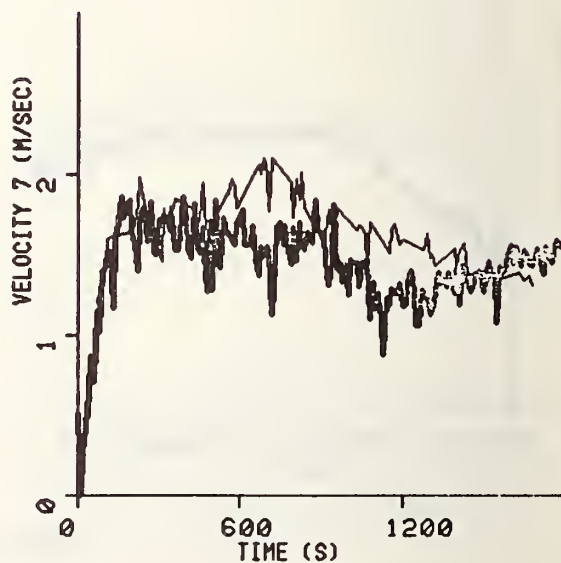
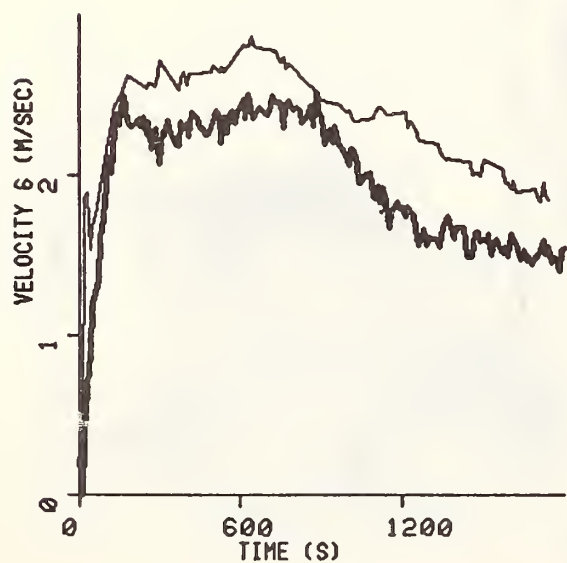
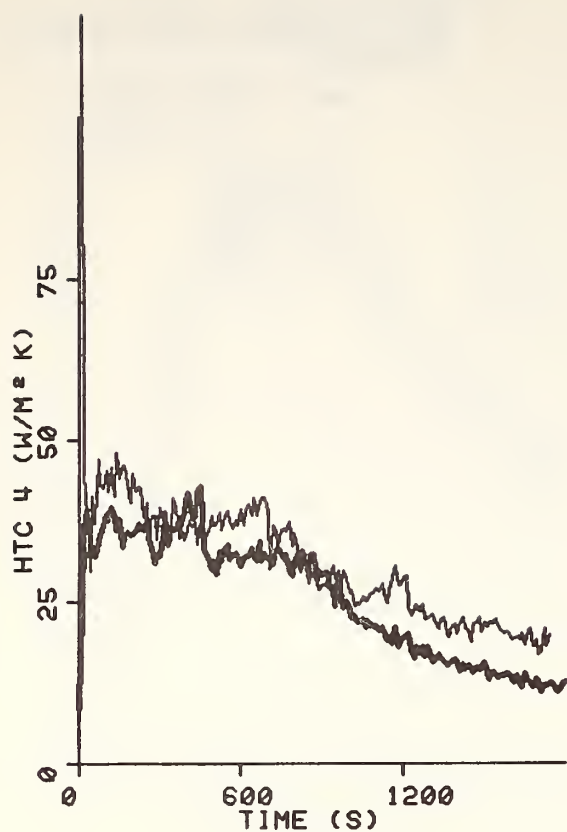


Figure 19b

CORRIDOR FIRE - 3 CRIES  
HEAT TRANSFER COEFFICIENT  
VELOCITY

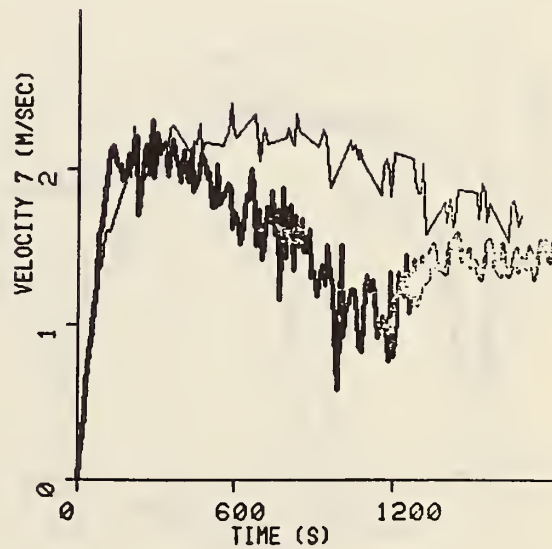
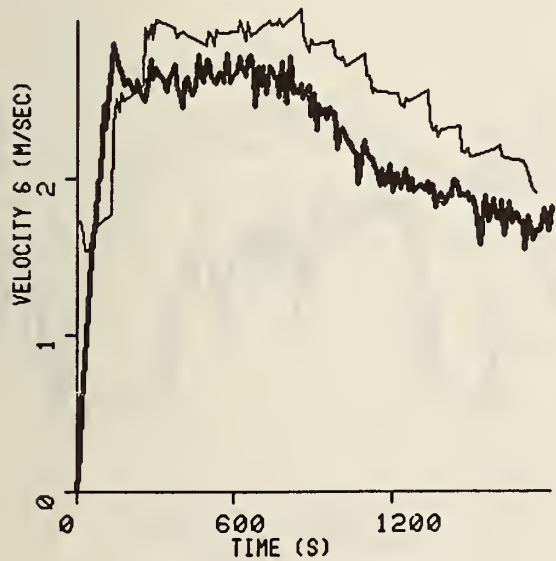
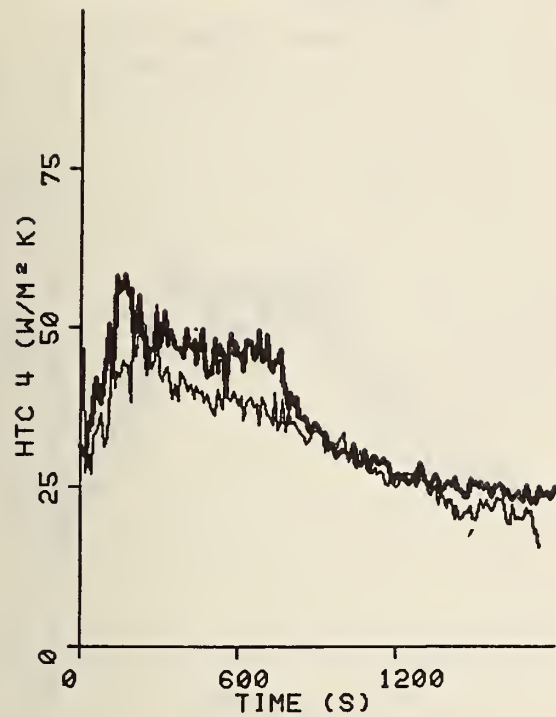


Figure 19c

CORRIDOR FIRE - 4 CRIBS  
HEAT TRANSFER COEFFICIENT  
VELOCITY

— FULL SCALE  
— 1/7 SCALE

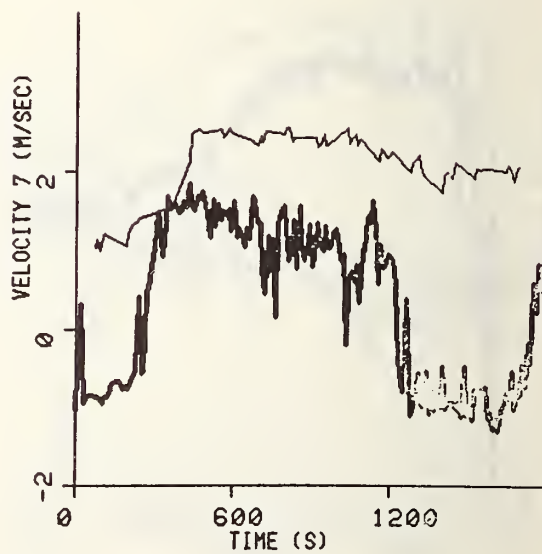
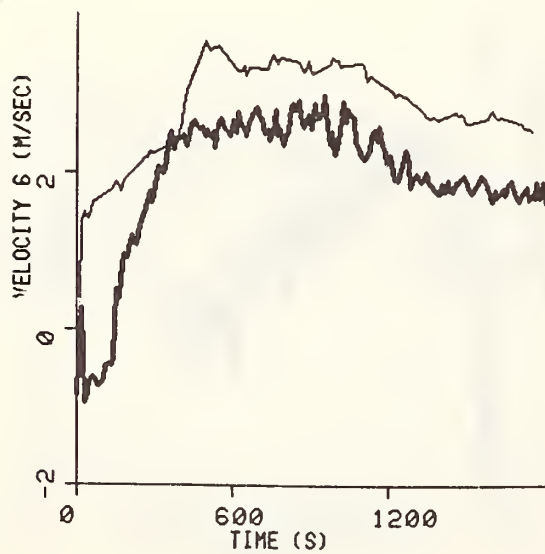
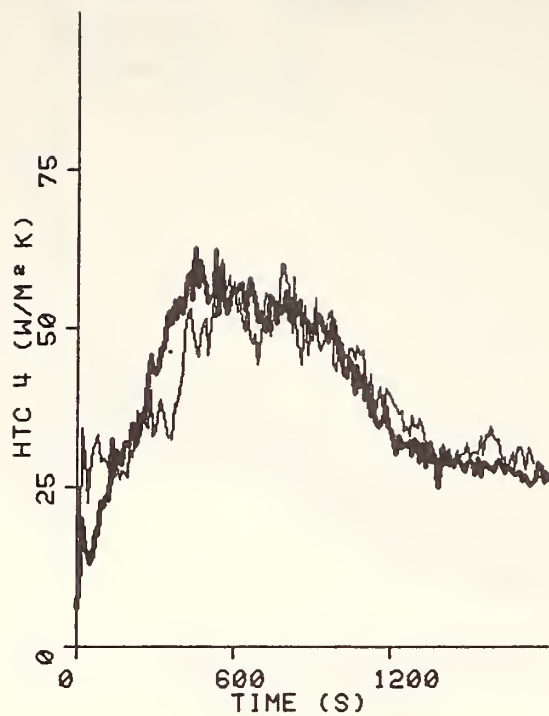


Figure 19d



CORRIDOR FIRE - 5 CRIES  
HEAT TRANSFER COEFFICIENT  
VELOCITY

— FULL SCALE  
— 1/7 SCALE

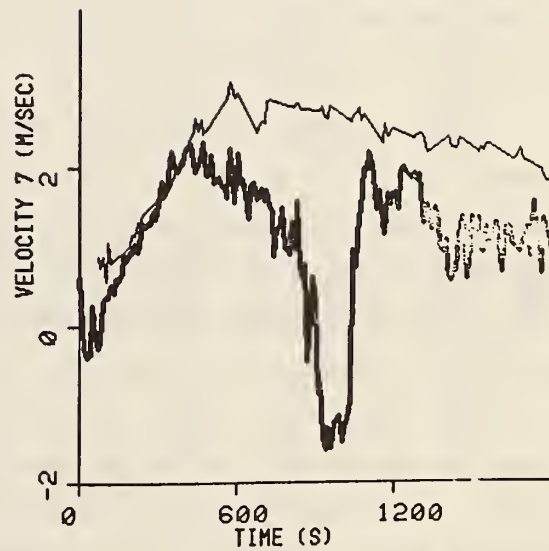
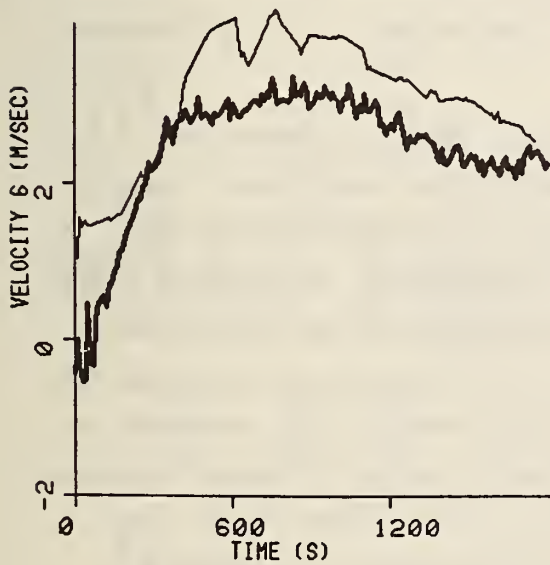


Figure 19e

## DESCRIPTION OF THE FULL-SCALE EXPERIMENTS

A total of nine experiments were run during a two-week period in June of 1974. All were run in the evening, and two runs were conducted on the same evening on occasion. The instrumentation for the corridor was described in the previous section and is shown in figure 1.










The adjoining room in which the primary fires were contained was 2.8 m high and 2.4 m x 2.6 m in floor area. Two small vents (18 cm x 35 cm) to permit additional inlet airflow into the burn room were located about 30 cm above the floor on opposite walls. These vents were either open or closed.

The motivation of the experiments was to determine the effect of the room vents, the effect of the fuel location, and the effect of an obstacle or floor fire at the room doorway.

The wood cribs were hemlock, and made of 3.8 cm square sticks, with 7.6 cm between the sticks, in 16 layers, having four sticks in each layer (except only two in the bottom layer). All the cribs were placed on a platform which covered most of the room floor and the platform was suspended a short distance above it. The platform was hung by a cable from a cooled load cell. The cribs were ignited with 250 g of heptane centered in a pan below each crib.

Table 3 gives a summary of experiments. The arrangement and quantity of fuel are given along with ventilation conditions. Experiments 8 and 9 were motivated by a behavior in the flow pattern that appeared to occur in the floor covering corridor fire experiments [11]. This was a decrease in the gas flow rate exchange at the room doorway which was speculated to have been caused by the advancing (opposing the airflow) floor fire. That is, as the floor covering fire increased in size, it would tend to become less affected by the air flowing along the floor. The consequences of this would be a taller floor flame, more forward heat transfer, and an increase in fire spread - a possible mechanism of rapid fire growth (flashover). Unfortunately because of a draft problem with some of the pressure transducers for the velocity

Table 3  
Summary of Experimental Conditions

Experiment Number	Date	Number and Arrangement of Cribs	Mass of Each Crib (kg)	Moisture Content of Fuel (%)	Other Fuel	Room Vent Condition	Other Ventilation Modifications
1	6/13/74		19.1, 19.5 19.1, 19.5	11.0-12.8	None	Open	None
2	6/14/74		19.5	12.8-13.0	None	Closed	None
3	6/14/74		19.1, 19.1 19.5, 19.5 19.5	11.8-13.5	None	Closed	None
4	6/18/74		19.1, 19.5	11.5-12.8	None	Closed	None
5	6/18/74		18.2, 19.5 19.5	10.5-17.2	None	Closed	None
6	6/19/74		19.1, 19.5 19.5, 19.5	11.8-13.5	None	Closed	None
7	6/20/74		19.1, 19.5 19.5, 20.0	-	None	Closed	None
8	6/26/74		19.1, 19.5 19.5, 20.0	12.0-15.0	None	Open	Room doorway blocked at 8 min with shield covering the bottom 0.97 m
9	6/27/74		19.1, 20.0 20.0, 20.0	-	1 m x 1 m carpet soaked with 500 ml of heptane ignited after 7 min from start of room fire	Open	None

probes, an illumination of this phenomena was not accomplished by the results of Experiments 8 and 9.

Except for the scaling analysis, the results of the full-scale experiments were not extensively analyzed. They will simply be documented here for the benefit of others who are concerned about particular features of this type of fire scenario.

The complete set of data are enclosed on microfiche with this report. Some features of the results will be discussed.

Figures 20, 21 and 22 show the temperature distribution on the corridor during the peak of the room fire for four cribs under three different conditions. Some observations are apparent. First, near the room doorway the temperature field is skewed by the effect of the doorway jet impinging on the corridor wall and turning down the corridor. Eventually, the temperature distribution in the hot gas flow becomes more uniform across the corridor width. The maximum corridor heating occurs for the condition of centered cribs with room vents closed. The increase in air supply with the vents open, lowers the temperatures overall. For the case of the corner location, the cribs burned at a slower rate, thus resulting in the lowest corridor temperature. This latter case could have had the opposite effect (over the centered, closed vent case) had the burning rate been the same. This would follow since it is expected that less air would be entrained into corner fires than room centered fires. Figure 23 shows these same effects in terms of heat flux to the corridor ceiling and floor.



## CONCLUSIONS

It has been shown that some scale model results could be accurately extrapolated to full-scale counterpart systems. However there can never be complete dynamic similarity in fire problems and this fact leads to uncertainty in the reliability of the scale model results. For the design conditions of these experiments, i.e. slowly varying fires, it was found that convective processes were modeled well. Since radiation effects were ignored in the scaling criteria, it was anticipated that results would be inaccurate when radiation becomes significant. However, the degree of disagreement in radiant flux could be estimated.

The full-scale experiments demonstrated that additional room ventilation and the location of the fuel load in the room, did affect the heating conditions of the corridor. The temperature field in the corridor appeared to be affected locally by geometry; but by 7 meters downstream of the room, the field became two-dimensional and invariant across the corridor width.



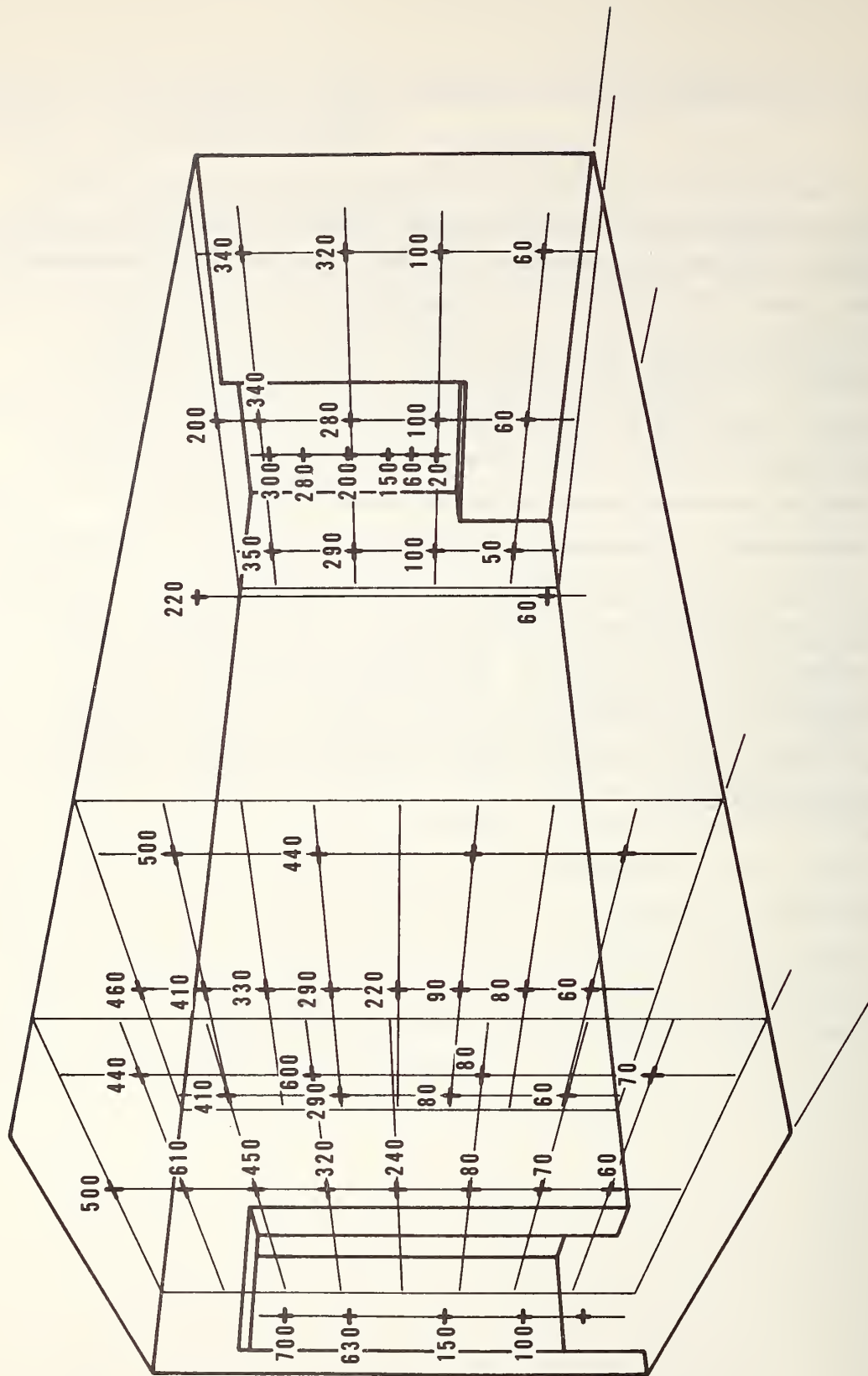


Figure 20. Peak average temperatures in °C for Run 1: 4 cribs, centered, vents open

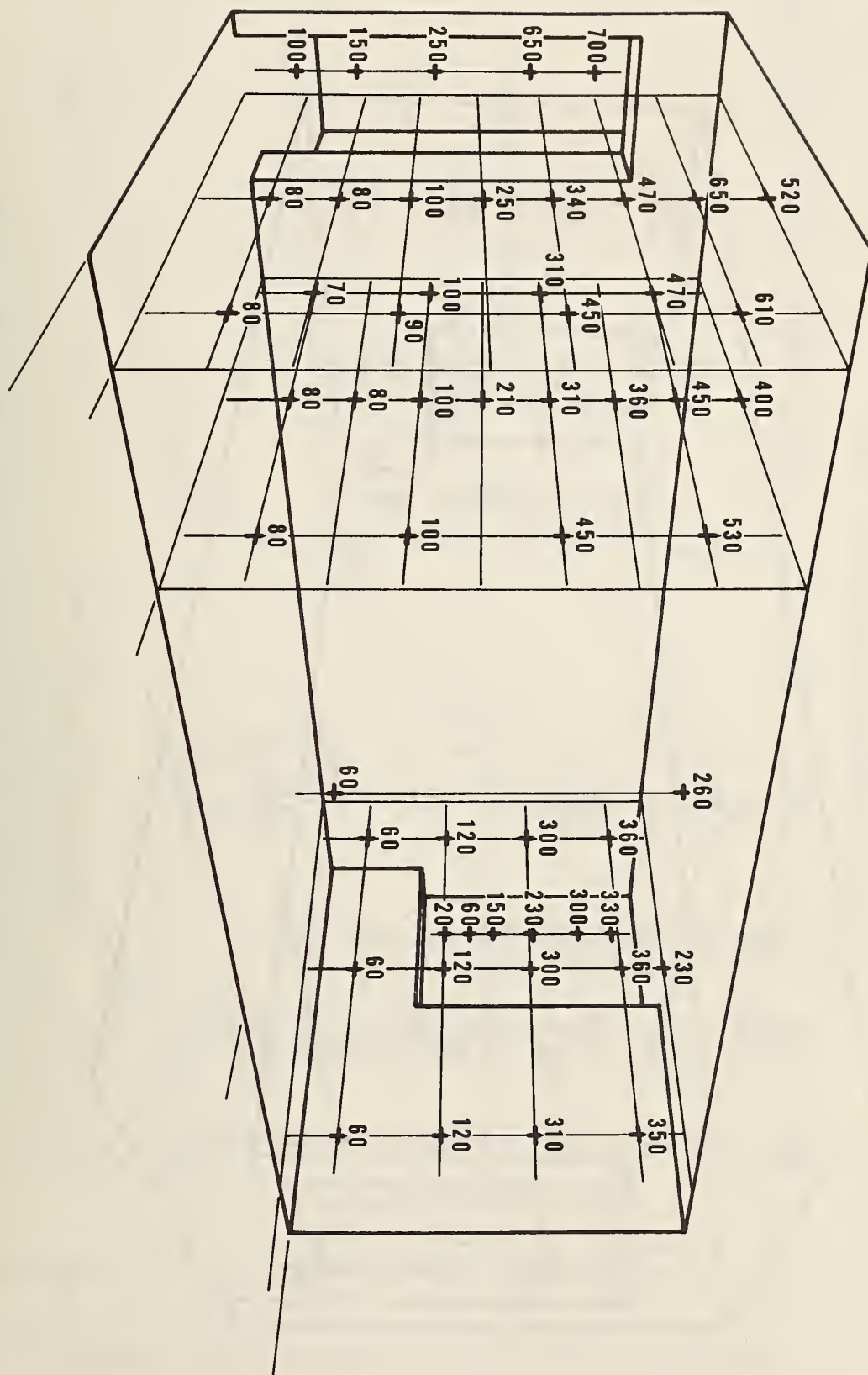


Figure 21. Peak average temperatures in °C for Run 6: 4 cribs, centered, vents closed

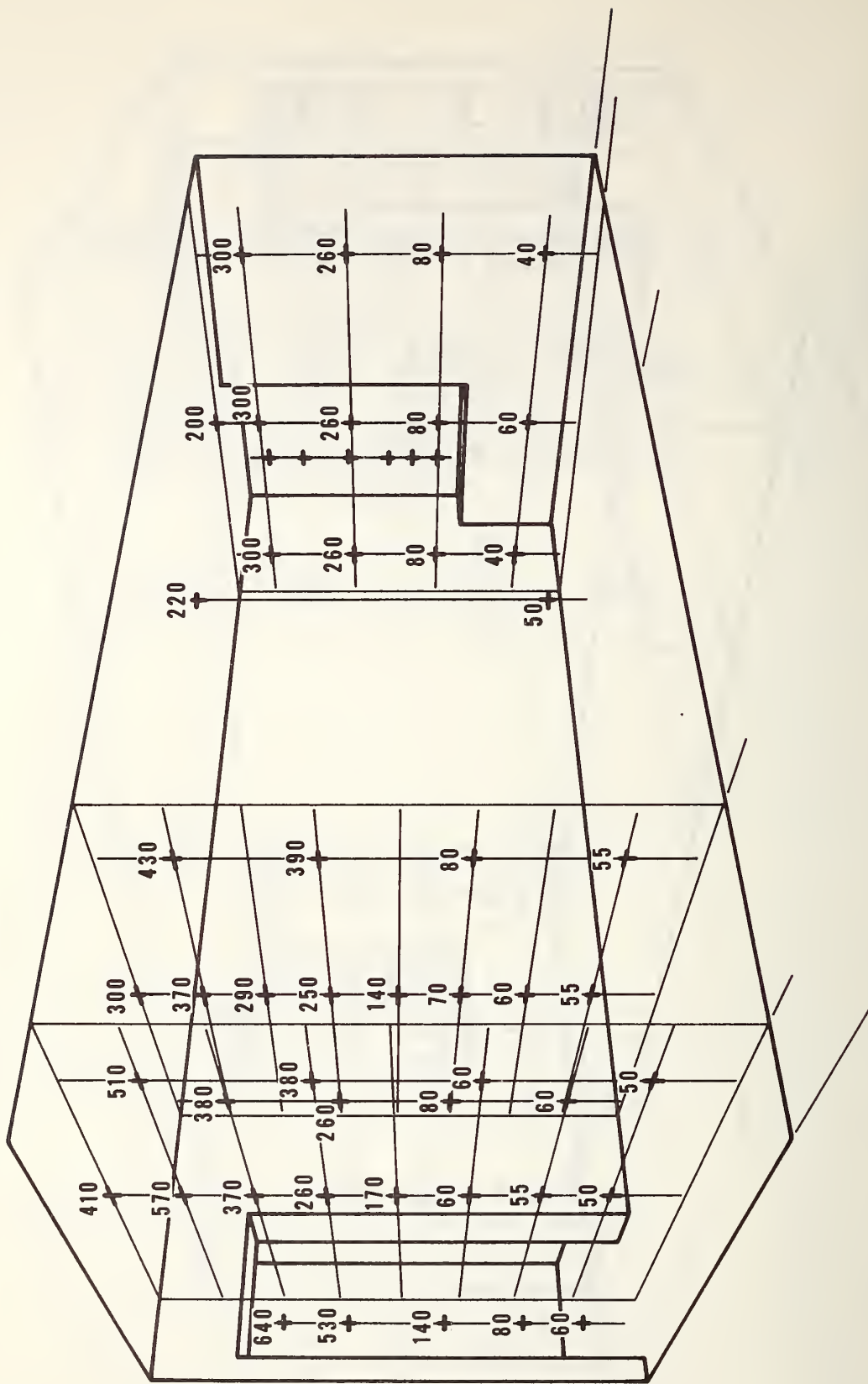


Figure 22. Peak average temperatures in °C for Run 7: 4 cribs, corner location, vents closed

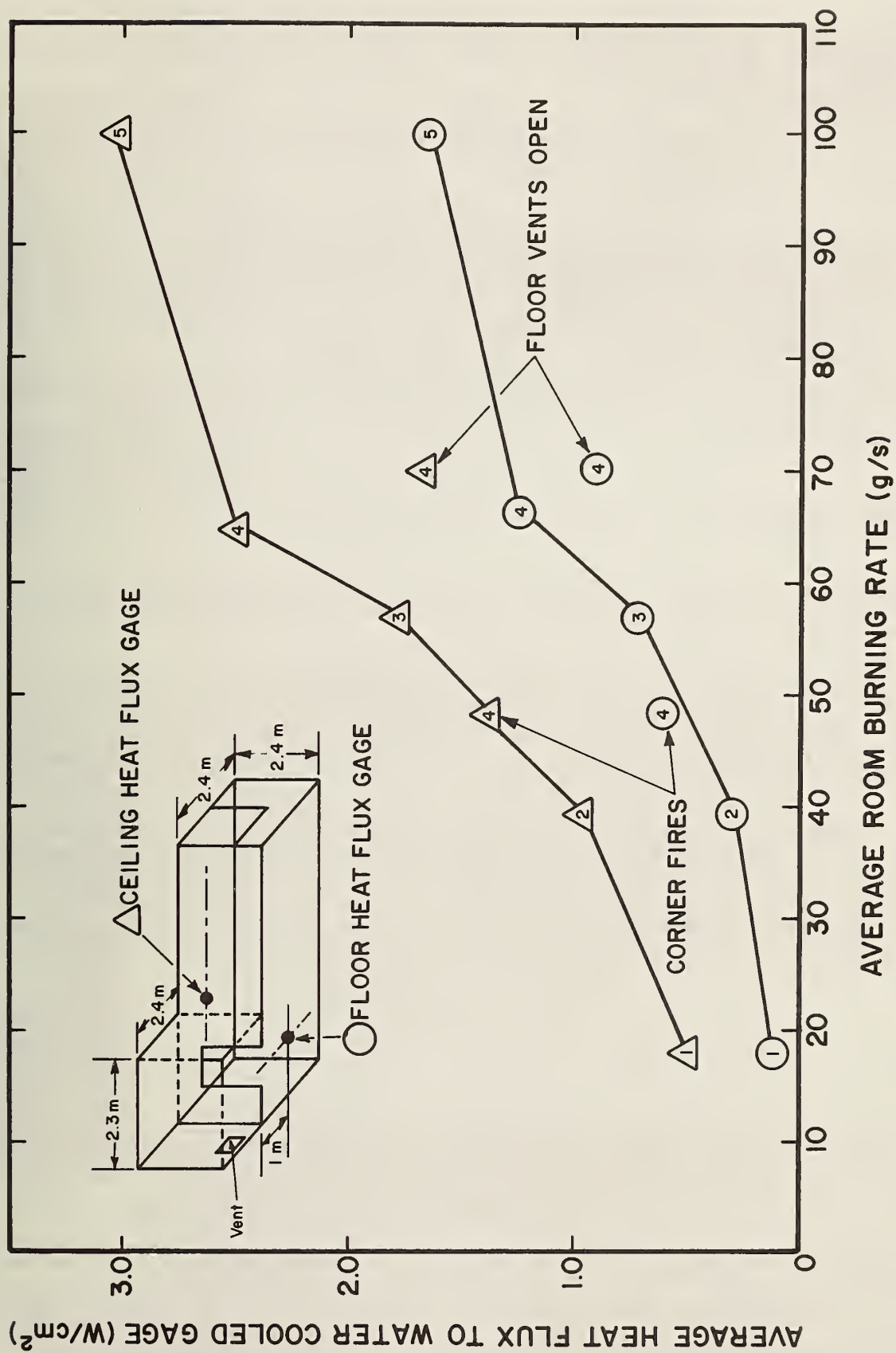


Figure 23. Corridor floor and ceiling heat transfer at maximum burning rate conditions



U.S. DEPT. OF COMM. BIBLIOGRAPHIC DATA SHEET	1. PUBLICATION OR REPORT NO. NBSIR 77- 1318	2. Gov't Accession No.	3. Recipient's Accession No.
4. TITLE AND SUBTITLE  The Impact of a Room Fire on a Corridor with Considerations of Fuel Load, Ventilation, and Scaling		5. Publication Date November 1977	
		6. Performing Organization Code	
7. AUTHOR(S) J. Quintiere, B. McCaffrey, T. Kashiwagi, K. Den Braven M. Harkleroad, J. Raines and W. Rinkinen		8. Performing Organ. Report No.	
9. PERFORMING ORGANIZATION NAME AND ADDRESS  NATIONAL BUREAU OF STANDARDS DEPARTMENT OF COMMERCE WASHINGTON, D.C. 20234		10. Project/Task/Work Unit No. 491	
		11. Contract/Grant No.	
12. Sponsoring Organization Name and Complete Address (Street, City, State, ZIP)  Same as No. 9		13. Type of Report & Period Covered Final Report	
		14. Sponsoring Agency Code	
15. SUPPLEMENTARY NOTES			
16. ABSTRACT (A 200-word or less factual summary of most significant information. If document includes a significant bibliography or literature survey, mention it here.)  <p>A study was conducted of heat transfer and temperature field imparted to a corridor by a room fire in order to assess the potential of fire spread along the corridor. Wood cribs were used as the fuel load which ranged from 20 to 120 kg. Also the effects of ventilation and fuel load location were examined. The results showed these effects to be significant.</p> <p>A corresponding scale model study was conducted using gas burners as a fuel supply. A scaling criteria was developed which emphasized the solid wall conductive and gas phase convective transport processes. As a result limitations were encountered at high temperature when radiation became more significant. In general the convective processes appeared to scale well and radiation limitations could be assessed through analysis.</p>			
17. KEY WORDS (six to twelve entries; alphabetical order; capitalize only the first letter of the first key word unless a proper name; separated by semicolons)  Corridors; fuel load; heat transfer; room fires; scaling; ventilation			
18. AVAILABILITY <input checked="" type="checkbox"/> Unlimited  <input type="checkbox"/> For Official Distribution. Do Not Release to NTIS  <input type="checkbox"/> Order From Sup. of Doc., U.S. Government Printing Office Washington, D.C. 20402, SD Cat. No. C13  <input checked="" type="checkbox"/> Order From National Technical Information Service (NTIS) Springfield, Virginia 22151		19. SECURITY CLASS (THIS REPORT)  UNCLASSIFIED	21. NO. OF PAGES  60
		20. SECURITY CLASS (THIS PAGE)  UNCLASSIFIED	22. Price  \$5.25